Chemistry Theses   Department of Chemistry

Summer 8-9-2022

Mechanistic Investigation of a Non-Catalytic Gating Residue in NADH:Quinone Oxidoreductase from Pseudomonas aeruginosa PA01

Bilkis Mehrin Moni
Georgia State University, bmoni1@student.gsu.edu

Follow this and additional works at: https://scholarworks.gsu.edu/chemistry_theses

Mechanistic Investigation of a Non-Catalytic Gating Residue in NADH:Quinone Oxidoreductase

from *Pseudomonas aeruginosa* PA01

By

Bilkis Mehrin Moni

Under the Direction of Giovanni Gadda, PhD

A Thesis Submitted in Partial Fulfillment of the Requirements for the Degree of

Master of Science

in the College of Arts and Sciences

Georgia State University

2022

ABSTRACT

NADH:quinone oxidoreductase from *Pseudomonas aeruginosa* PAO1 (NQO, PA1024, EC 1.6.5.9) is a recently reclassified flavin-dependent enzyme that catalyzes the two-electron reduction of a wide variety of quinones to hydroquinone using NADH as an electron donor. The two-electron reduction of quinone plays a detoxification role in *P. aeruginosa* by avoiding the formation of semiquinone radicals. The previously solved crystal structure of the NQO demonstrated that the substrate-binding site of NQO is formed by a small entrance consisting of a flexible βα loop 3 (residue 75-86). Q80 in loop 3 switches between an open conformation without NAD^+ bound and a close conformation with NAD^+ bound. In this study, Q80 was mutated to glycine, leucine, or glutamate through site-directed mutagenesis to investigate the role of Q80 in binding and catalysis in NQO. The results showed that Q80 residue participates in substrate NADH binding in the active site of NQO.

INDEX WORDS: NADH:quinone oxidoreductase, Flavin-dependent enzyme, NADH, Quinones, Loop 3, Substrate binding, Detoxification.

Mechanistic Investigation of a Non-Catalytic Gating Residue in NADH:Quinone Oxidoreductase

from *Pseudomonas aeruginosa* PA01

by

Bilkis Mehrin Moni

Committee Chair: Giovanni Gadda

Committee: Samer Gozem

Dabney Dixon

Electronic Version Approved:

Office of Graduate Services

College of Arts and Sciences

Georgia State University

August 2022

DEDICATION

I dedicate my thesis work to my late father, Md. Belal Uddin and elder brother Md. Shah Alam for their unconditional love and support all of their life.

ACKNOWLEDGEMENTS

TABLE OF CONTENTS

LIST OF TABLES

LIST OF FIGURES

LIST OF SCHEMES

LIST OF ABBREVIATIONS

NQO, NADH:quinone oxidoreductase from *P. aeruginosa*; *Q80*, glutamine 80; *Q80G*, glutamine 80 mutation to glycine; *Q80L*, glutamine 80 mutation to leucine; *Q80E*, glutamine 80 mutation to glutamate; *BQ*, 1,4-benzoquinone; *CoQo*; 2,3-dimethoxy 5-methyl 1,4-benzoquinone; *juglone*, 5-hydroxy 1,4-naphthoquinone, *WT*, wild Type, *QRs*, quinone reductases, NQO2, N-ribosyl dihydro-nicotinamide:quinone oxidoreductase.

CHAPTER 1.

1 INTRODUCTION

1.1 NAD(P)H:quinone reductases

Flavin-dependent quinone reductases (QRs) provide the strict two-electron reduction of the quinones to its hydroquinone. QRs prevent the generation of semiquinone, which is prone to react with molecular dioxygen leading to the generation of superoxide radicals.[1] QRs are known to cause oxidative stress in prokaryotic and eukaryotic organisms. Hence, QRs have a protective role against quinone-related oxidative cell damage. Since handling oxidative stress is vital for both prokaryotic and eukaryotic organisms, flavin-dependent QRs have been identified in bacteria, fungi, plants, and mammals.[1] These enzymes utilize a flavin cofactor, either FMN or FAD, to transfer a hydride from an electron donor, such as NAD(P)H, to a quinone substrate.[2] The family of flavin-dependent quinone reductase shares a flavodoxin-like structure and reaction mechanisms pointing towards a common evolutionary origin.[2]

Originally, QRs were classified as DT-diaphorases; the enzymes that utilize both NADH and NADPH as a source of reducing equivalents.[2] The term diaphorases was usually used to describe enzymes (mostly flavoproteins) capable of transferring electrons from pyridine nucleotides to electron acceptors.[2] The first DT-diaphorase reported by Ernster and Navazio is now known as mammalian NAD(P)H:quinone oxidoreductase (NQO1).[3] However, the acronym "NQO" has been traditionally confined to QRs from mammalian sources.[4] The mammalian QRs act as a molecular switch that control the lifespan of transcription factor p53 and, thus, contributes to the development of cell transformation and apoptosis.[3]

Several QRs utilize NADH and NADPH as a electrons donors, such as NsfB from *Escherichia coli* and Lot6p from *Saccharomyces cerevisiae*,[5, 6] whereas others prefer NADH

(AzoA from *Enterococcus faecalis*)[7] or NADPH (YhdA from *Bacillus subtilis*).[8] Conversely, mammalian N-ribosyl dihydro-nicotinamide (NRS):quinone oxidoreductase (NQO2) cannot use NADH and NADPH as sources of electrons. Instead, it employs N-ribosyl- and N-alkyl-dihydro-nicotinamide as a reducing substrate.[3] The preference for oxidizing substrates of QRs is far more complicated. The structure and size of the active sites of NQO1, NQO2, and Lot6p suggest these enzymes evolved to accept a wide range of ring-containing compounds. Naturally occurring quinones comprising vitamin K derivatives (menaquinone and phylloquinone), coenzyme Q (ubiquinone), and dopaquinone were also found to be substrates for mammalian QRs.[2]

1.2   NAD(P)H:quinone oxidoreductase from *Pseudomonas aeruginosa*

NAD(P)H:quinone oxidoreductases (NQOs) play a fundamental antioxidant role in detoxifying quinones from the intracellular ambiance in *P. aeruginosa*.[9] The physiological significance of NQOs utilizing NAD(P)H as the reducing substrate is not well understood compared to the relevance of the quinone reduction.[3] The importance of NQOs using NAD(P)H as the reducing substrate was investigated by analyzing the genome context of NQOs.[10] The operon encoding for NQOs also contains a hypothetical acyl-CoA dehydrogenase, an enoyl-CoA hydratase, and a porin suggesting NQOs translated with these enzymes play a role in the β-oxidation pathway in *P. aeruginosa* PA01.[8]

1.2.1   PA1024 and PA0660

Two genes, *Pa1024* and *Pa0660* in the GenBank, were originally annotated based on bioinformatics as hypothetical nitronate monooxygenase in *P. aeruginosa* PA01 (NMOs).[11] NMOs have more than 5000 genes in the GenBank.[11, 12] NMOs are a flavin-dependent enzymes that catalyze the oxidation of metabolic poison propionate-3-nitronate (P3N) and other nitronate analogs.[13] The classification as an NMO was uncontested until the structural motifs characteristic

of class I NMOs were established.[10] The comparison of structural motifs showed that PA1024 does not contain any conserved structural sequence characteristics of class I NMOs.[10] Therefore, the PA0124 function was reevaluated through the mechanistic investigations, which revealed that enzyme does not exhibit NMO activity; instead uses NADH, but not NADPH and quinones as an oxidoreductase.[10] In 2018, PA1024 was reclassified as an NADH:quinone oxidoreductase (NQO, EC 1.6.5.9), which may participate in maintaining the NAD^+/NADH ratio for catabolism of fatty acid in *P. aeruginosa* PA01.[10] Six conserved motifs in the primary sequence of PA1024 along with structural and biochemical data, define a new class of NADH:quinone oxidoreductases (**Table 1.1**) that includes more than 490 hypothetical proteins in the GenBank.[10]

PA0660 was previously annotated as a hypothetical NMO based on bioinformatics.[11] However, no biochemical evidence was available at the transcript and protein level. PA0660 shares only 27% and 29% sequence identity and modest overall sequence similarities of 38% and 42% with PaNMO and PA1024, respectively.[11] Additionally, PA0660 does not possess the consensus motifs of class I and class II NMOs or PA1024, suggesting the enzyme may have different catalytic activity. It was tentatively identified as a member of a new class of NADPH:quinone reductase enzymes.[11] PA0660 has a non-covalently bound FMN in the active site. The enzyme is reduced with NADPH or NADH with marked preference for NADPH and oxidized with a wide range of quinones (**Table 1.1**).[11] Six conserved motifs were identified in the protein sequence of PA0660, which are different from PaNMO and PA1024, and are conserved in more than 1000 proteins erroneously annotated as hypothetical NMOs in the GenBank database.[11]

1.2.2   PA1225

The *P. aeruginosa* PA01 complete genome has been sequenced, and more than 2000 genes of the 5570 open reading frames were annotated as a "hypothetical protein" in 2016.[14, 15] One of

the hypothetical proteins in *P. aeruginosa,* PA1225, was annotated as NAD(P)H dehydrogenase with a flavodoxin like fold.[16] PA1225 has ~20-30% sequence similarities with human NQO1 and NQO2.[17] In 2018; biochemical evidence validated the annotation of the *Pa1225* gene as encoding a NAD(P)H:quinone reductase. PA1225 is a FAD-dependent quinone:reductase which operates through ping-pong bi-bi steady-state kinetic mechanisms (**Table 1.1**).[12] NADPH is the preferred reducing substrate, whereas NADH was also used with a 40-fold lower efficiency.[12] Single and double-ring quinones are both suitable oxidizing substrates for the PA1225.[12]

Table 1.1: NAD(P)H:quinone oxidoreductase from *P. aeruginosa* PA01

Gene	Cofactor	Reducing agent	Reaction	Protein fold	Reference
PA1024	FMN	NADH	Ping-pong bi-bi	TIM-barrel	10
PA0660	FMN	NADPH/NADH	Ping-pong bi-bi	TIM-barrel	11
PA1225	FAD	NADPH/NADH	Ping-pong bi-bi	Flavodoxin	12

1.3 *P. aeruginosa* **NADH:quinone oxidoreductase (NQO)**

The protein PA1024 from *P. aeruginosa* PAO1 was previously annotated in the GenBank and PDB databases as a nitronate monooxygenase;[18] structural, biochemical, and bioinformatic studies have successively shown it to be a NADH:quinone oxidoreductase.[19] The NQO from *P. aeruginosa* is an FMN-dependent enzyme that employs a ping-pong bi-bi mechanism in turnover by first reducing the flavin via a hydride transfer from NADH, then a hydride transfer from the flavin to the quinone (**Scheme 1.1**).[1, 9, 19]
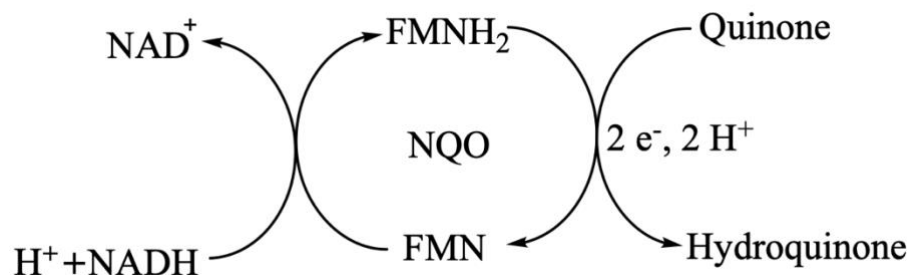
Scheme 1.1: Reaction catalyzed by NQO from *P. aeruginosa* with NADH and quinone.

The enzyme can accomplish the two-electron reduction by receiving two electrons from NADH to form the reduced flavin and then transferring those two electrons to the quinone (**Scheme 1.1**). The two-electron transfer between the NQO and the quinone may reduce quinone toxicity resulting from a single electron transfer of the NQO to the quinone.[20] A single electron transfer onto a quinone creates a free radical that can promote highly reactive oxygen species (ROS), leading to tissue degradation and cell death (**Figure 1.1**). NQO may play an essential role in the cellular detoxification of *P. aeruginosa* by avoiding the generation of harmful quinone species that lead to cytotoxicity.[9, 20] Genome context analysis suggests that NQO may also maintain an appropriate $[NADH]/[NAD^+]$ ratio for the catabolism of fatty acids in *P. aeruginosa*.[1, 21]
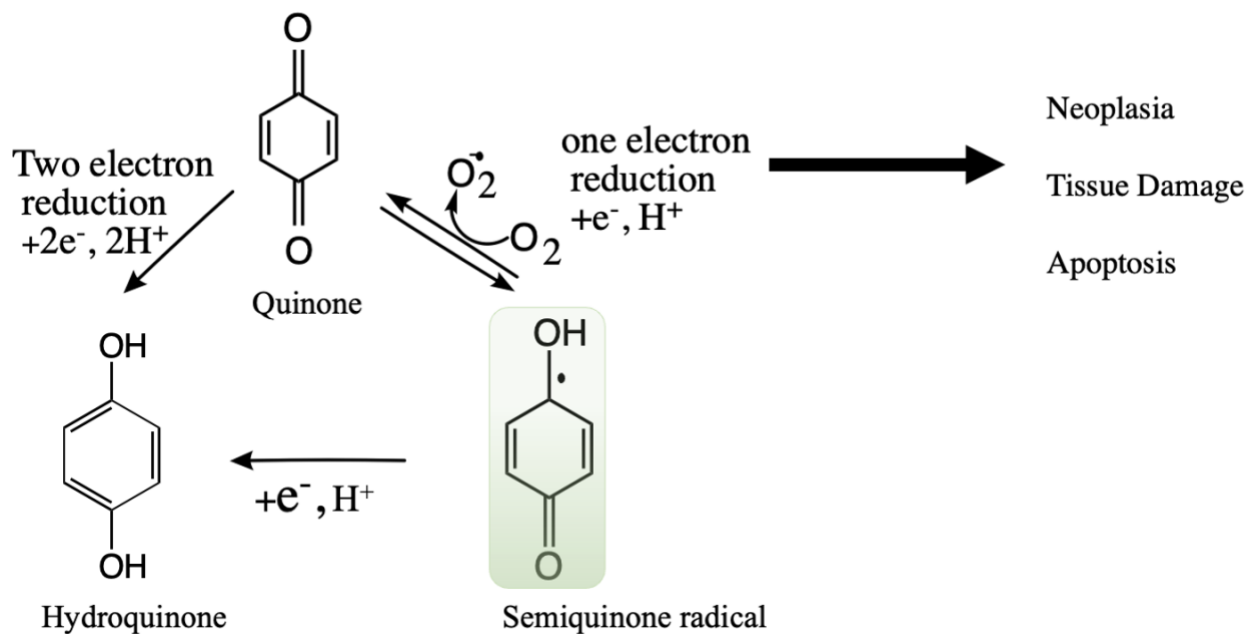
Figure 1.1: One and two-electron reductions of quinones. A two-electron reduction of oxidized quinone achieves hydroquinone formation. One-electron reduction of quinones creates the semiquinone radical. Modified from reference [1].

NQO from *P. aeruginosa* shares little overall sequence similarity with flavin-dependent NAD(P)H:quinone oxidoreductases, such as eukaryotic NAD(P)H:quinone oxidoreductase 1 (NQO1), eukaryotic NQO2, lot6p from *S. cerevisiae*,[6] or the tryptophan repressor binding protein from *E. coli* (WrbA).[22] Most NAD(P)H:quinone reductases (NQOs) have a TIM-barrel fold, typically a flavodoxin-like fold, including the well-characterized NQO1 and NQO2.[1] The enzyme NQO from *P. aeruginosa* has a strict specificity for NADH with virtually no reactivity with NADPH. The best quinone substrates for NQO are benzoquinone and naphthoquinone.[19]

1.4   Substrates of NQO

1.4.1 Quinones-Oxidizing substrates

Quinones are six-membered cyclic, unsaturated compounds that contain two carbonyl groups, resulting in a fully conjugated cyclic dione.[23] The carbonyl groups can be adjacent or separated by a vinylene group.[23, 24] Quinones are abundant organic compounds in the environment and prokaryotic and eukaryotic cells.[3] The simplest single ring form of quinone is 1,4-benzoquinone, whereas the double ring form is 5-hydroxy-1,4-naphthoquinone (**Figure 1.2**) will be studied in this thesis.

1,4-benzoquinone ┊┊ **5-hydroxy-1,4-naphthoquinone**
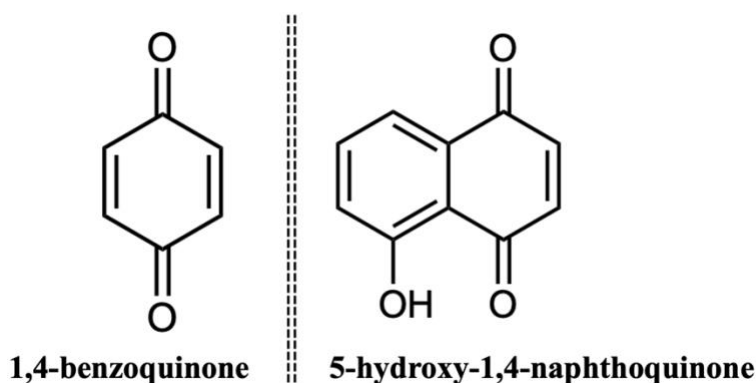
Figure 1. 2: Structure of 1,4-benzoquinone, and 5-hydroxy-1,4-napthoquinone. The single ring form of quinone is 1,4-benzoquinone, and the double ring form is 5-hydroxy-1,4-naphthoquinone.

Quinones are pervasive and participate in various reactions, most notably in the electron transport chain in the form of Coenzyme Q_0.[25, 26] The substrate 1,4-benzoquinone is used as a chemical intermediate, a polymerization inhibitor, an oxidizing agent, and a chemical reagent in the dye, textile, tanning, and cosmetic industries.[26] Exposure to high levels of benzoquinone via inhalation and skin absorption in humans results in eye irritation and dermatitis.[26, 27] In animal studies, oral exposure to benzoquinone has high acute toxicity.[28] Naturally, benzoquinone is used by the bombardier beetle along with hydrogen peroxide as a chemical spray to deter predators.[27]

The substrate 5-hydroxy-1,4-naphthoquinone is a secondary metabolite in plants with allelopathic properties naturally produced by the black walnut (*Juglans nigra*). It is toxic to other plants and insect herbivores, and bacteria; *Pseudomonas putida*, a soil bacterium found in black walnut roots, metabolizes juglone and uses it as a carbon source for energy production.[29-33] Due to its cytotoxic properties, 5-hydroxy-1,4-naphthoquinone has been investigated as an anti-cancer agent.[33, 34]

1.4.2   NADH-Reducing substrates

Nicotinamide adenine dinucleotide (NAD^+) is a coenzyme central to the metabolism of living organisms. The coenzyme NAD^+ consists of two nucleotides, an adenine nucleobase and nicotinamide joined through their phosphate groups (**Figure 1.2**). It exists in both an oxidized NAD^+ and reduced NADH form (**Figure 1.2**). The enzyme NQO uses NADH as a reducing substrate and will be studied in this thesis.

The NADH and NAD^+ play critical roles in energy metabolism, cell death, mitochondrial functions, immune function, and various cellular function, including regulation of calcium homeostasis and gene expression.[35] NAD^+ and NADH might affect the aging processes and oxidative damage-mediated diseases due to their effect on cellular antioxidation capacity.[35, 36] A variety of enzymes with varying functions uses NADH as a substrate or a cofactor. Significant classes include oxidoreductase such as NAD(P)H:quinone oxidoreductases (NQOs), azoreductases such as glutathione reductases, [37] and dehydrogenases such as lactate dehydrogenase and glutamate dehydrogenase.[38, 39]
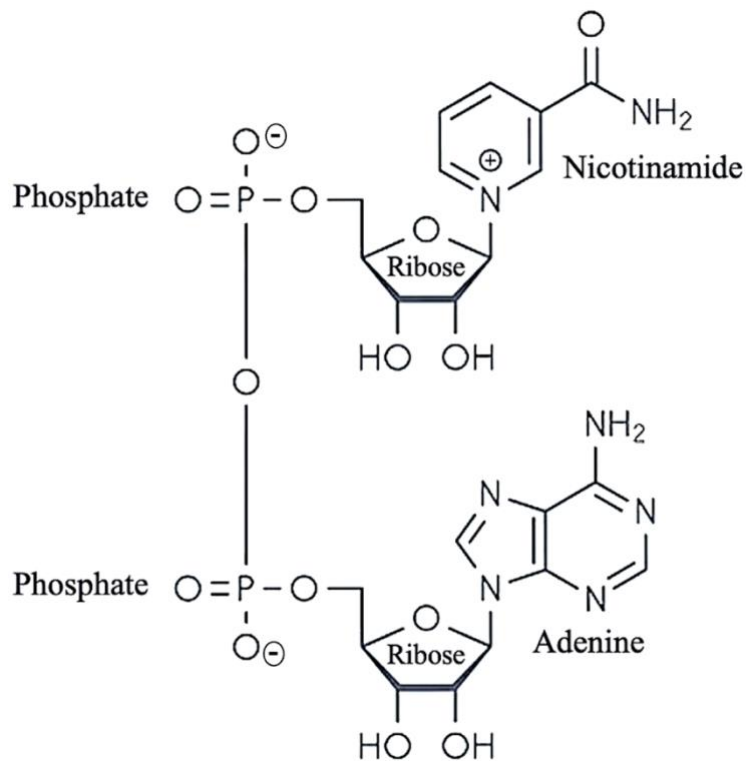
Figure 1.3: Structure of NADH. It consists of two nucleotides, an adenine nucleobase and nicotinamide joined through their phosphate groups.

1.5 Three-dimensional structure of NQO

The three-dimensional structure of NQO in a complex with NAD$^+$ was determined previously by X-ray crystallography at 2.2 Å resolution (**Figure 1.4**).[40] The oxidized form of substrate NAD$^+$ binds in a folded conformation at the interface of the TIM-Barrel domain (M^1-P^{211} and E^{299}-V^{328}) and extended domain (I^{212}-Asp^{298}) of the enzyme (**Figure 1.4**).[40]
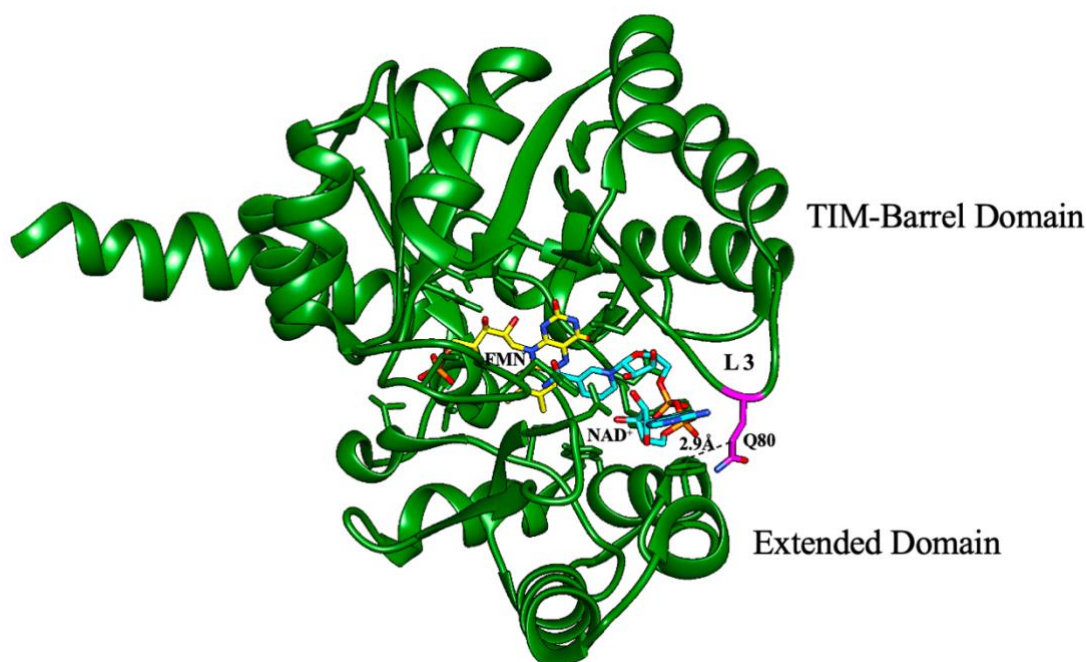
Figure 1. 4: The overall structure of NQO with NAD⁺ (PDB: 6E2A). The NQO structure is shown in a cartoon representation. The NAD⁺ and cofactor FMN are shown as sticks and colored cyan and yellow, respectively. The TIM-barrel domain's residue interacts with the extended domain's residue, creating an NAD⁺ binding pocket.

A comparison of NAD⁺ bound NQO with the ligand-free structure revealed a conformational change of a mobile loop (Loop 3, residues 75-86), part of the NAD⁺-binding pocket. The residues P78, P82, and P84 provide internal rigidity to loop 3, whereas Q80 serves as an active site latch that secures the NAD⁺ within the binding pocket. The adenine moiety of NAD⁺ appears to π–π stack with Y261. A steric constraint occurs between the adenosine ribose of NAD⁺, P78, and Q80, which controls the strict specificity of NQO for NADH.[40]
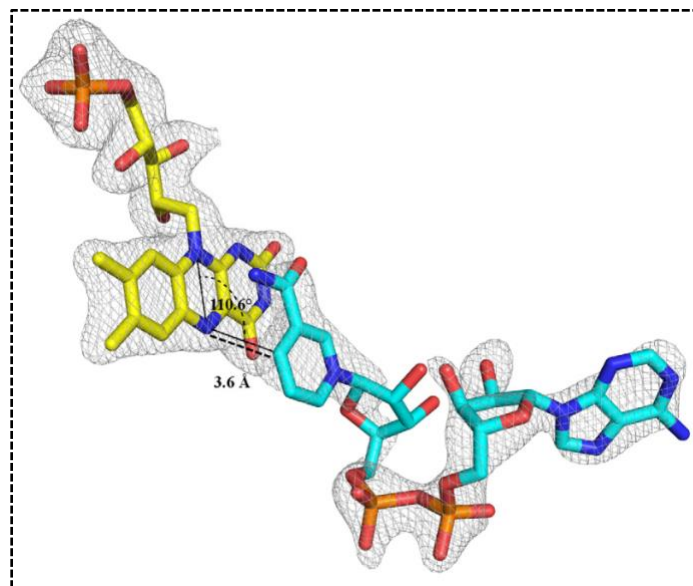
Figure 1.5: The binding mode of NAD$^+$ to NQO. The NAD$^+$ carbons are in cyan sticks, and FMN carbon is in yellow. The dashed line indicates the distance between the C$_4$ atom of the nicotinamide and the N$_5$ atom of the FMN. The solid line defines the angle between the N$_5$ and N$_{10}$ atom of the FMN and the C$_4$ atom of the nicotinamide. Taken from reference *[26]* with author permission.

The crystal structure of NQO has shown that the C$_4$ atom of the nicotinamide is 3.6 Å away from the N$_5$ atom of FMN, with a donor/acceptor angle of 110.6^0 for the atoms involved in the hydride transfer reaction (**Figure 1.5**). The proximity and donor/acceptor are thought to represent a binding mode relevant to facile hydride transfer from the nicotinamide of NAD$^+$ to the N5 atom of FMN. However, the nicotinamide ring of the NAD$^+$ does not appear to directly π–π stack with the pyrazine ring of FMN.[40] One FMN molecule was found to be non-covalently bound to the active site pocket of NQO. Structural analysis of NQO suggests the cofactor forms a hydrogen bonds between phosphate moiety and the protein backbone amide atom of A150, G180, G201, and T202 to remain bound within the protein.[18]
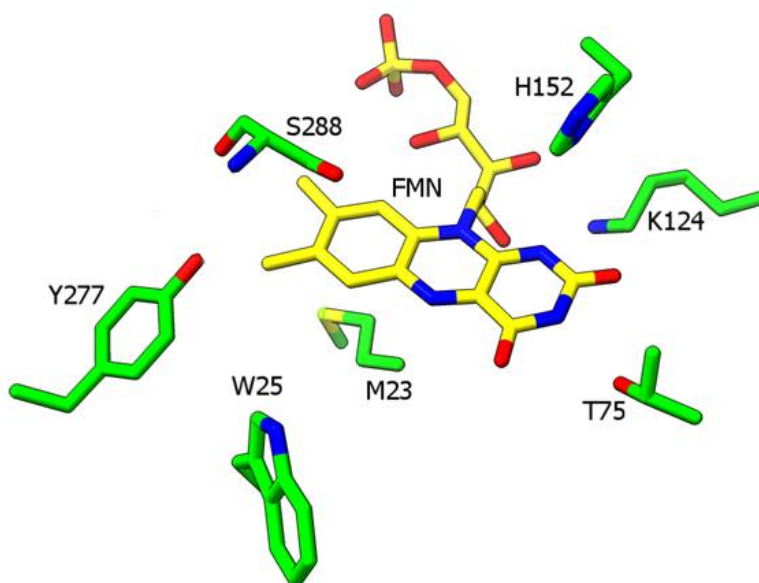
Figure 1.6: Active site topology of NQO (PDB: 2GJL). The active site of NQO depicts the position of the FMN cofactor and key active site residues. FMN carbon atoms are yellow, and the carbon atoms of protein are lime green. Oxygen and nitrogen atoms are red and blue, respectively.

The active site frameworks of NQO showed H152 present above the flavin and S288 near the C7/C8 methyl's of the flavin. K124 is located near the N1 of NQO, and M23 is positioned behind the re-face of flavin. Additionally, T75 is below the flavin and hydrophilic residues near the flavin's N1-C2(O) locus (**Figure 1.6**). The active site residues of NQO differed from the active site residues of mammalian NQO1 and NQO2. NQO from *P. aeruginosa* displays several differences with respect to mammalian NQOs. NQO from *P. aeruginosa* contains FMN, whereas mammalian NQOs use FAD. NQO prefers NADH, whereas NQO1 can utilize NADH and NADPH with similar efficacy. NQO1 and NQO2 use azo dyes as a substrate, whereas NQO cannot reduce azo dyes.

1.6 Active site gate

The catalytic efficiency of an enzyme depends on the active site of the enzyme. The amino acid residues and their atoms in the active site are fine-tuned to bind ligands efficiently and stabilize the reaction intermediates.[41] A gate consists of individual residues, loops, secondary structural elements, or domains switching between open and closed conformations. Gates control the passage of substrates, products, ions, and solvent molecules in and out of the active site of an enzyme.[42] The substrate-binding site of NQO is formed by a small entrance consisting of a flexible βα loop 3 (residue 75-86). Loop 3 adopts two conformations depending on whether the substrate is present or not in the active site (**Figure 1.7**).[40]
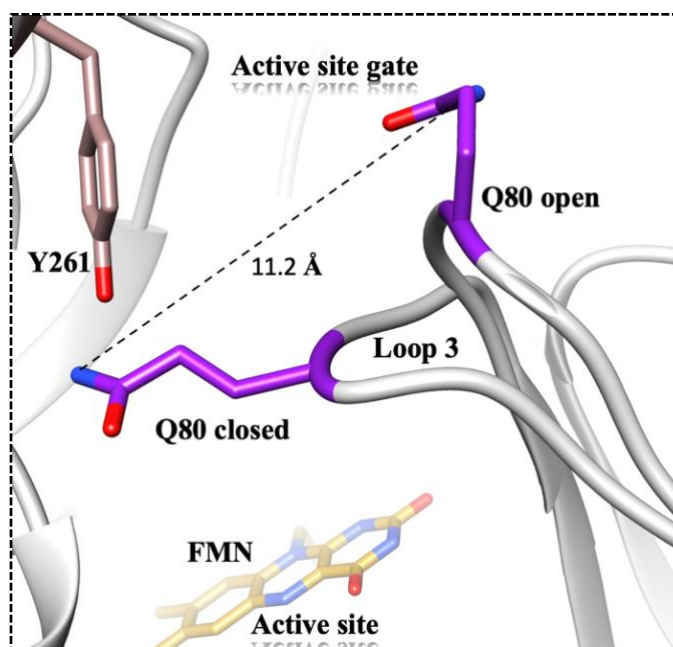
Figure 1.7: The active site topology of NQO shows the open and close conformation of the active site gate. The Q80 residue represents purple, Y261 in rose gold, and FMN in yellow color. The distance between Q80 residue in the open and closed conformation is 11.2 Å.

A significant movement of loop 3 is observed. In the ligand-free conformation, Q80 points away from the active site in ligand-free conformation (**Figure 1.7**). In the ligand bound conformation, in contrast, the side chain of Q80 moves toward the substrate-binding site and establishes a hydrogen bond interaction with Y261 in the ligand-bound conformation. In the loop 3 region, Q80 adopts two conformations shown in Figure 1.6. Q80 acts as a hypothetical "door" that seals the active site entrance of NQO by forming a hydrogen bond with Y261 upon NAD^+ binding (**Figure 1.8**). Therefore, the door keeps the NAD^+ secure in the active site while the O1 and O2 atom of the adenine phosphate moiety of NAD^+ forms a hydrogen bond interaction with the backbone amides of Q80 (3.4 Å) in loop 3 (**Figure 1.8**).
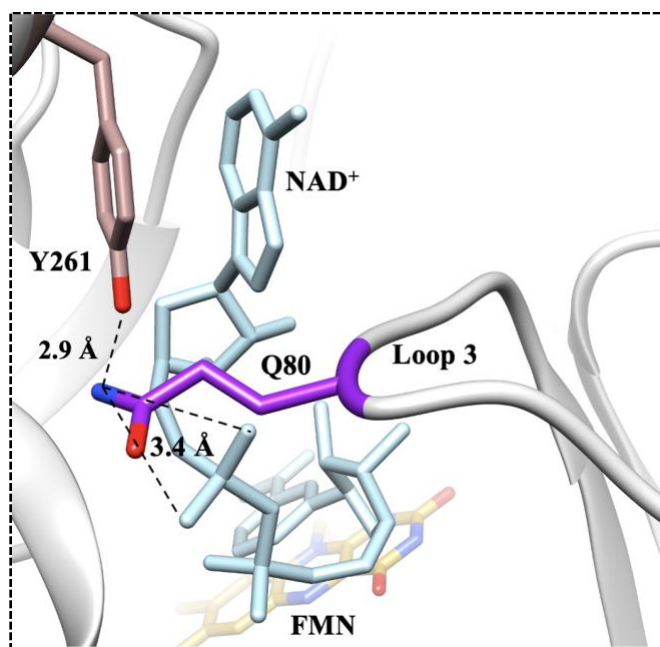
Figure 1.8: NQO-NAD^+ complex (PDB: 6e2a). The gate of NQO becomes closed upon NAD^+ binding. The residue Q80 in loop 3 interacts with Y261, creating a gate that secures NAD^+ in the active site of NQO. The Q80 residue is purple, Y261 is rose gold, NAD^+ is cyan and FMN is yellow.

Three proline residues in loop 3 provide structural rigidity to the loop and allow for the proper gate conformation to be sampled.[43] The proline 78 (P78) on loop 3 among all three prolines is conserved. [40] The structural rigidity of conserved P78 modulates the gate conformation of NQO (**Figure 1.9**). The 2'-hydroxyl of the adenine ribose of NAD$^+$ establishes a hydrogen bond with the backbone C=O of P78 (3.1Å). [40] In a previous study, the mutation of P78 with glycine decreased the rate of the dissociation constant for substrate binding (K_d).[43] Therefore, P78 is important for substrate NADH binding in the active site of NQO.
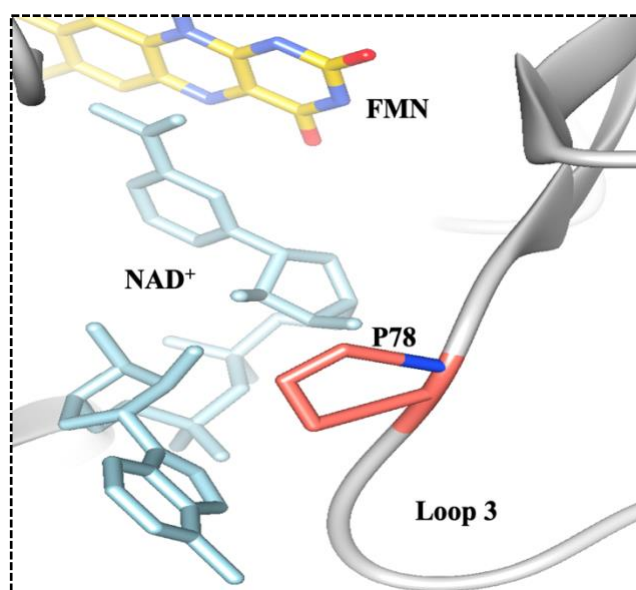
Figure 1. 9: Conserved P78 provides structural rigidity of NQO upon NAD$^+$ bound. The P78 residue in loop 3 is orange, NAD$^+$ is cyan, and FMN is yellow.

A similar flexible loop, located at the entrance of the substrate-binding site, was reported in D-amino acid oxidase (DAAO) as an "active site lid" that may control the substrate binding and product release.[44] The Glucose-Methanol-Choline structural family, including choline oxidase, glucose oxidase, cholesterol oxidase, pyranose 2-oxidase, and cellobiose dehydrogenase

flavoprotein domain, displays the same "loop and lid" feature.[44, 45] Therefore, the shape and feature of the active site gate in NQO may play a significant role in substrate binding and product release.

1.7   Specific goals

This thesis investigates the effect of a gating residue in βα loop 3 for substrate binding and flavin reduction in NQO using site-directed mutagenesis, protein expression, and purification, UV-visible absorption spectroscopy, steady-state kinetics, and reductive-half reaction. The Q80 in loop 3 is hypothesized to act as a gating residue, allowing the gate of NQO to adopt conformational changes necessary to facilitate substrate binding. The Q80 of NQO might interact with Y261 residue, which seals the active site gate and secures NADH in the active site upon NADH binding. Therefore, we hypothesize the gating Q80 is required to maintain proper gate conformations that modulate the rate of substrate association in NQO. The results of these studies are presented in the second chapter, along with the mechanistic interpretation of the role played by Q80 in substrate NADH binding and enzymatic catalysis.

1.8   References

[1] Deller, S., Macheroux, P., and Sollner, S. (2007) Flavin-dependent quinone reductases, *Cell. Mol. Life Sci. 65*, 141.

[2] Ernster, L. (1987) DT diaphorase: a historical review, *Chem. Scr. 27*, 1-13.

[3] Bianchet, M. A., Faig, M., and Amzel, L. M. (2004) Structure and mechanism of NADPH: quinone acceptor oxidoreductases (NQO), *Meth. Enzymol. 382*, 144-174.

[4] Vasiliou, V., Ross, D., and Nebert, D. W. (2006) Update of the NAD(P)H: quinone oxidoreductase (NQO) gene family, *Hum. Genomics 2*, 1-7.

[5] Zenno, S., Koike, H., Tanokura, M., and Saigo, K. (1996) Gene cloning, purification, and characterization of NfsB, a minor oxygen-insensitive nitroreductase from *Escherichia coli*, similar in biochemical properties to FRase I, the major flavin reductase in *Vibrio fischeri*, *J. Biochem. 120*, 736-744.

[6] Sollner, S., Nebauer, R., Ehammer, H., Prem, A., Deller, S., Palfey, B. A., Daum, G., and Macheroux, P. (2007) Lot6p from *Saccharomyces cerevisiae* is an FMN-dependent reductase with a potential role in quinone detoxification, *Fed. Europ. Biochem. Soc. J. 274*, 1328-1339.

[7] Chen, H., Wang, R.-F., and Cerniglia, C. E. (2004) Molecular cloning, overexpression, purification, and characterization of an aerobic FMN-dependent azoreductase from *Enterococcus faecalis*, *Protein Expr. Pur. 34*, 302-310.

[8] Deller, S., Sollner, S., Trenker-El-Toukhy, R., Jelesarov, I., Gübitz, G. M., and Macheroux, P. (2006) Characterization of a thermostable NADPH:FMN oxidoreductase from the mesophilic bacterium *Bacillus subtilis*, *Biochemistry 45*, 7083-7091.

[9] Atia, A., Alrawaiq, N., and Abdullah, A.(2014) A review of NAD(P)H:Quinone oxidoreductase 1 (NQO1); A multifunctional antioxidant enzyme, *J. Appl. Pharm. Sci. 4*, 118-122.

[10] Ball, J., Salvi, F., and Gadda, G. (2016) Functional Annotation of a Presumed Nitronate Monoxygenase Reveals a New Class of NADH:Quinone Reductases*, *J. Biol. Chem. 291*, 21160-21170.

[11] Reis, R. A., Salvi, F., Williams, I., and Gadda, G. (2019) Kinetic investigation of a presumed nitronate monooxygenase from *Pseudomonas aeruginosa* PAO1 establishes a new class of NAD (P) H:quinone reductases, *Biochemistry 58*, 2594-2607.

[12] Flores, E., and Gadda, G. (2018) Kinetic characterization of PA1225 from *Pseudomonas aeruginosa* PAO1 reveal a new NADPH:quinone reductase, *Biochemistry 57*, 3050-3058.

[13] Francis, K., Smitherman, C., Nishino, S. F., Spain, J. C., and Gadda, G. (2013) The biochemistry of the metabolic poison propionate 3-nitronate and its conjugate acid, 3-nitropropionate, *IUBMB life 65*, 759-768.

[14] Winsor, G. L., Griffiths, E. J., Lo, R., Dhillon, B. K., Shay, J. A., and Brinkman, F. S. (2016) Enhanced annotations and features for comparing thousands of Pseudomonas genomes in the Pseudomonas genome database, *Nucleic Acids Res. 44*, D646-D653.

[15] LaBaer, J., Qiu, Q., Anumanthan, A., Mar, W., Zuo, D., Murthy, T. V., Taycher, H., Halleck, A., Hainsworth, E., and Lory, S. (2004) The *Pseudomonas aeruginosa* PA01 gene collection, *Genome Res. 14*, 2190-2200.

[16] (2017) UniProt: the universal protein knowledgebase, *Nucleic Acids Res. 45*, D158-D169.

[17] Chen, C., Huang, H., and Wu, C. H. (2017) Protein bioinformatics databases and resources, *Protein Bioinform.*, 3-39.

[18] Atia, A., Alrawaiq, N., and Abdullah, A. (2014) A review of NAD(P)H: Quinone oxidoreductase 1 (NQO1); A multifunctional antioxidant enzyme, *J. Appl. Pharm. Sci. 4*, 118-122.

[19] Zhao, Q., Yang, X. L., Holtzclaw, W. D., and Talalay, P. (1997) Unexpected genetic and structural relationships of a long-forgotten flavoenzyme to NAD (P) H:quinone reductase (DT-diaphorase), *Proc. Natl. Acad. Sci. 94*, 1669-1674.

[20] Deller, S., Macheroux, P., and Sollner, S. (2007) Flavin-dependent quinone reductases, *Cell. Mol. Life Sci. 65*, 141.

[21] Ha, J. Y., Min, J. Y., Lee, S. K., Kim, H. S., Kim, K. H., Lee, H. H., Kim, H. K., Yoon, H.-J., and Suh, S. W. (2006) Crystal structure of 2-nitropropane dioxygenase complexed with FMN and substrate: Identification of the catalytic base, *J. Biol. Chem. 281*, 18660-18667.

[22] Ball, J., Salvi, F., and Gadda, G. (2016) Functional annotation of a presumed nitronate monooxygenase reveals a new class of NADH: quinone reductases, *J. Biol. Chem. 291*, 21160-21170.

[23] Li, R., Bianchet, M. A., Talalay, P., and Amzel, L. M. (1995) Correction: The Three-Dimensional Structure of NAD(P)H:Quinone Reductase, a Flavoprotein Involved in Cancer Chemoprotection and Chemotherapy: Mechanism of the Two-Electron Reduction, *Proc. Natl. Acad. Sci.*, p 10815.

[24] Sollner, S., Nebauer, R., Ehammer, H., Prem, A., Deller, S., Palfey, B. A., Daum, G., and Macheroux, P. (2007) Lot6p from *Saccharomyces cerevisiae* is an FMN-dependent reductase with a potential role in quinone detoxification, *FEBS. J. 274*, 1328-1339.

[25] Patridge, E. V., and Ferry, J. G. (2006) WrbA from *Escherichia coli* and *Archaeoglobus fulgidus* is a NAD(P)H:quinone oxidoreductase, *J. Bacteriol. 188*, 3498-3506.

[26] Kim, H. S., and Huber, K. C. (2007) Simple purification (desalting) procedure to facilitate structural analysis of an alkali-solubilized/neutralized starch solution by intermediate-pressure size-exclusion chromatography, *J. Agri. Food Chem. 55*, 4944-4948.

[27] Kruger, N. J. (2009) The Bradford method for protein quantitation, *Protein Protocol handbook*, 17-24.

[28] Fujita, T., Shiota, K., Yoshikawa, J., Ogawa, S., and Aoyagi, H. (2019) Simple method for analyzing the purity of protease-containing samples by acid-treatment SDS-PAGE, *J. Biosci. Bioeng. 128*, 630-635.

[29] Quaye, J. A., and Gadda, G. (2020) Kinetic and Bioinformatic Characterization of d-2-Hydroxyglutarate Dehydrogenase from *Pseudomonas aeruginosa* PAO1, *Biochemistry 59*, 4833-4844.

[30] Verselis, V. K., Trelles, M. P., Rubinos, C., Bargiello, T. A., and Srinivas, M. (2009) Loop gating of connexin hemichannels involves movement of pore-lining residues in the first extracellular loop domain, *J. Biol. Chem. 284*, 4484-4493.

[31] Melcher, K., Ng, L.-M., Zhou, X. E., Soon, F.-F., Xu, Y., Suino-Powell, K. M., Park, S.-Y., Weiner, J. J., Fujii, H., and Chinnusamy, V. (2009) A gate–latch–lock mechanism for hormone signaling by abscisic acid receptors, *Nature 462*, 602-608.

[32] Hastie, K. M., Liu, T., Li, S., King, L. B., Ngo, N., Zandonatti, M. A., Woods, V. L., de la Torre, J. C., and Saphire, E. O. (2011) Crystal structure of the Lassa virus nucleoprotein–RNA complex reveals a gating mechanism for RNA binding, *Proc. Natl. Acad. Sci. 108*, 19365-19370.

[33] Beckstein, O., and Sansom, M. S. (2006) A hydrophobic gate in an ion channel: the closed state of the nicotinic acetylcholine receptor, *Phy. Biol. 3*, 147.

[34] Chang, H.-R., and Kuo, C.-C. (2008) The activation gate and gating mechanism of the NMDA receptor, *J. Neurosci. 28*, 1546-1556.

[35] Dreyer, I., and Blatt, M. R. (2009) What makes a gate? The ins and outs of Kv-like K+ channels in plants, *Trends. Plant Sci. 14*, 383-390.

[36] Price, K. L., and Lummis, S. C. (2004) The role of tyrosine residues in the extracellular domain of the 5-hydroxy-tryptamine 3 receptor, *J. Biol. Chem. 279*, 23294-23301.

[37] Stenberg, G., Board, P., Carlberg, I., and Mannervik, B. (1991) Effects of directed mutagenesis on conserved arginine residues in a human class alpha glutathione transferase, *Biochem. J. 274*, 549-555.

[38] Chen, K., Robinson, A. C., Van Dam, M. E., Martinez, P., Economou, C., and Arnold, F. H. (1991) Enzyme engineering for nonaqueous solvents. II. Additive effects of mutations on the stability and activity of *subtilisin E* in polar organic media, *Biotechnol. Prog. 7*, 125-129.

[39] Huang, L., Ma, H. M., Yu, H. L., and Xu, J. H. (2014) Altering the substrate specificity of reductase CgKR1 from *Candida glabrata* by protein engineering for bioreduction of aromatic α-keto esters, *Ad. Synth.Catal. 356*, 1943-1948.

[40] Meng, X., Yang, L., Liu, Y., Wang, H., Shen, Y., and Wei, D. (2021) Identification and Rational Engineering of a High Substrate-Tolerant Leucine Dehydrogenase Effective for the Synthesis of L-*tert*-Leucine, *Chem.Cat. Chem. 13*, 3340-3349.

[41] Roberge, M., Shareck, F., Morosoli, R., Kluepfel, D., and Dupont, C. (1998) Site-directed mutagenesis study of a conserved residue in family 10 glycanases: Histidine 86 of xylanase A from *Streptomyces lividans*, *Protein Eng. 11*, 399-404.

[42] Wongsantichon, J., Harnnoi, T., and Ketterman, A. J. (2003) A sensitive core region in the structure of glutathione S-transferases, *Biochem. J. 373*, 759-765.

[43] Ball, J., Reis, R. A. G., Agniswamy, J., Weber, I. T., and Gadda, G. (2019) Steric hindrance controls pyridine nucleotide specificity of a flavin-dependent NADH:quinone oxidoreductase, *Protein Sci. 28*, 167-175.

[44] Tsou, C. L. (1993) Conformational flexibility of enzyme active sites, *Science 262*, 380-381.

[45] Gora, A., Brezovsky, J., and Damborsky, J. (2013) Gates of Enzymes, *Chem. Rev. 113*, 5871-5923.

[46] Dratch, B.D, Iyer, A., Ouedraogo, D., Ball, J., Weber, I., Hamelberg, D. and Gadda, G. (2022) Increased Mobility of Loop 3 Widens Gate Dynamics and Alters Substrate Capture Based on Substrate Size in NADH:Quinone Oxidoreductase, *Unpublished Manuscript*.

[47] Terry-Lorenzo, R. T., Chun, L. E., Brown, S. P., Heffernan, M. L., Fang, Q. K., Orsini, M. A., Pollegioni, L., Hardy, L. W., Spear, K. L., and Large, T. H. (2014) Novel human D-amino acid oxidase inhibitors stabilize an active-site lid-open conformation; Biosci. *Rep. 34*.

[48] Quaye, O., Lountos, G. T., Fan, F., Orville, A. M., and Gadda, G. (2008) Role of Glu312 in binding and positioning the substrate for the hydride transfer reaction in choline oxidase, *Biochemistry 47*, 243-256.

CHAPTER 2

2 MUTATION OF A DISTAL GATING RESIDUE MODULATES SUBSTRATE AFFINITY IN NADH:QUINONE OXIDOREDUCTASE

2.1 Abstract

Enzymes require flexible regions to adopt multiple conformations during catalysis. The flexible regions of enzymes, include gates that modulates the passage of molecules in and out of the active site of the enzyme. The enzyme PA1024 from *Pseudomonas aeruginosa* PA01 is a recently discovered flavin-dependent NADH:quinone oxidoreductase (NQO, EC 1.6.5.9). Glutamine 80 (Q80) in loop 3 (residues 75-86) of NQO is ~15 Å away from the flavin and creates a gate that seals the active site through a hydrogen bond with tyrosine 261 (Y261) upon NADH binding. In this study, Q80 was mutated to glycine, leucine, or glutamate to investigate the significance of Q80 in NADH binding in the active site of NQO. The UV-visible absorption spectrum revealed that the mutation of Q80 minimally affects the spectral properties of the enzyme. The anaerobic reductive half-reaction of the NQO-mutants yielded a $\geq$60-fold increase in the K_d value for NADH compared to the WT enzyme. However, the k_{red} values for NADH were similar across all enzymes (~25 s^{-1}). The NQO-Q80G enzyme acquired no reactivity for the possible substrate NADPH. Steady-state kinetics with NQO-mutants and NQO-WT at varying concentrations of NADH and 1,4-benzoquinone established a $\leq$5.3-fold decrease in the k_{cat}/K_{NADH} value. Moreover, there was no significant difference in the k_{cat}/K_{BQ} (~1×10^6 M^{-1}s^{-1}) and k_{cat} (~24 s^{-1}) values in NQO-mutants and NQO-WT. These results are consistent with a decreased binding affinity for NADH with minimal effect on the rate of hydride transfer from NADH to flavin upon Q80 mutation.

2.2 Introduction

Enzymes are very efficient catalysts for the functioning of living organisms and require some degree of flexibility for catalytic activity.[1] The flexibility enables them to alternate between active and inactive conformational states during a catalytic cycle. Flexible protein regions are dynamic enzyme portions that participate in a conformational switch.[2-4] Gates are examples of flexible regions in enzymes.[1, 3] A gate consists of individual residues, loops, secondary structural elements, or domains switching between open and closed conformations.[5] Gates control the passage of substrates, products, ions, and solvent molecules in and out of the protein.[1, 6-8] The various interactions of gating residues can control the size and properties of ligands that pass through the gate. Interestingly, the high variability of gating residues can restrict specific substrates or result in selectivity for other substrates.[9] Thus, gating residues play a vital mechanistic role in controlling substrate access and product release by forming a path between the active site pocket and the bulk solvent.[6-8, 10, 11]

The high rate of evolution of the gating residues and their specific location within the protein structure makes them attractive protein engineering targets.[1, 5, 12-15.] For successful protein engineering, mutation of gating residues must not be detrimental to protein function.[9-13] Three observations about gating residues support the idea of their attractiveness for protein engineering.[1, 12, 16-18] Firstly, the mutation of a gating residue is not detrimental to protein function, as gating residues are often spatially separated from the active site. Secondly, the gating residues control the opening and closing of the access pathway; thus, mutations can affect ligand exchange resulting in altered enzyme activity and substrate selectivity. Finally, modification of gating residues can modulate the solvent accessibility to the active site, affecting substrate binding and product release.[19] Additionally, site-directed mutagenesis of bulky gating residues to smaller residues

sometimes provides previously hindered bulky substrates access to the active site cavity.[9-13] In a previous study, the D285I and D285Q mutations in toluene-4-monooxygenase from *Pseudomonas mendocina* improved its ability to oxidize the large and bulky substrates 2-phenyl ethanol or methyl p-tolyl sulfide by 8 and 11-fold, respectively, and the D285S mutation improved the rate of styrene oxidation by 1.7-fold.[15]
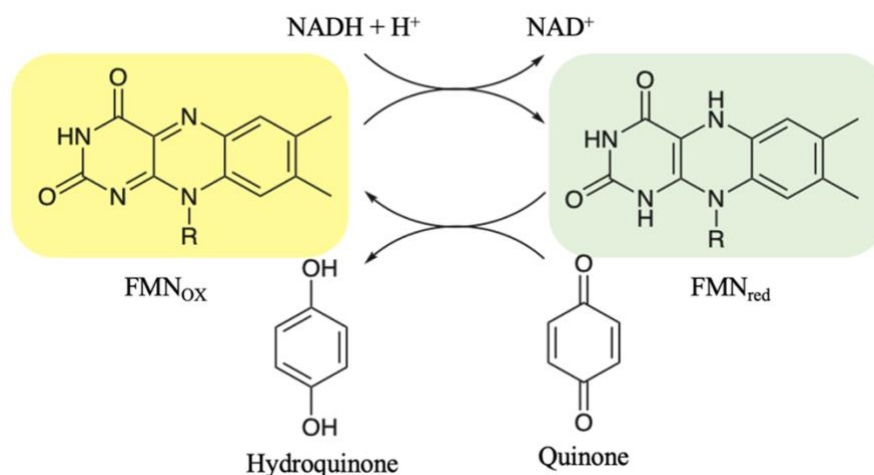
Scheme 2.1: Reaction mechanism of NQO with 1,4-benzoquinone as a substrate.

The enzyme PA1024 from *P. aeruginosa* PA01 is a recently discovered FMN-dependent NADH:quinone oxidoreductase (NQO).[20] NQO utilizes a ping-pong bi-bi mechanism in its catalytic turnover by first reducing the bound flavin via a hydride transfer from NADH, followed by a hydride transfer from the flavin to the quinone (**Scheme 2.1**).[20-26] The enzyme has a marked preference for NADH over NADPH, unlike the eukaryotic homolog NQO1 that can use NADPH as a substrate.[21, 27] Genome context analysis suggests that NQO serves a dual function in the cell by detoxifying quinones and maintaining an [NAD$^+$]/[NADH] ratio favorable for fatty acid catabolism in *P. aeruginosa*.[20-22, 26, 28] NQO consists of a TIM-barrel domain and an extended domain, where a hinge region connects the two domains to form the active site pocket.[29] TIM-

barrel domains are usually composed of 8 parallel β-strands at the center of the fold and 8 α-helices with βα and αβ loops connecting the secondary structures.[30, 31] Extended domains, on the other hand, are formed by combining secondary structures that directly interact with the central chain atoms.[32, 33] The βα loops of the TIM-barrel domain are located at the C-terminal ends of the β-strands, pointing towards the enzyme active site, which is crucial for the activity of TIM-barrel-containing enzymes.[31, 34]
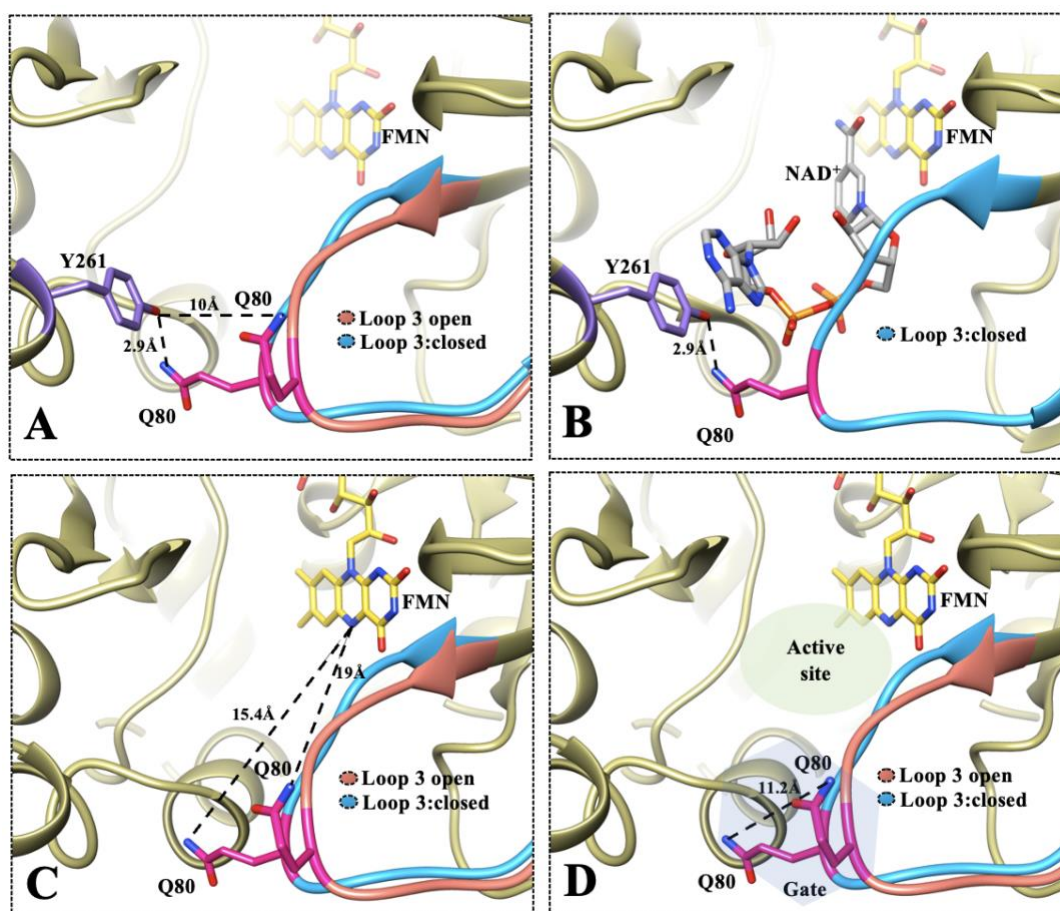
Figure 2. 1: Gating the active site in NQO-WT (PDB: 6E2A and 2GJL). (A) Formation and breaking of gating interactions between Q80 with Y261 in open and closed conformations; (B) Gating of NQO active site by Q80 and Y261 upon NAD$^+$ binding; (C) Distance of Q80 from the active site flavin in both open and closed conformations; (D) Active site topology of NQO showing gating residue Q80 in open and closed conformations. The PDB files were analyzed using the USCF Chimera visualizing software.[56]

Previously solved crystal structures of NQO reveal that the βα loop 3 (residues 75-86) of the TIM-barrel domain of NQO is displaced by 5.5 Å towards the active site in the presence of NAD$^+$.[29] Loop 3 is therefore proposed to act as a gate that stabilizes the enzyme-substrate complex by forming hydrogen bond interactions with the extended domain of NQO.[29] Q80 of loop 3 shows spatial variability in the ligand-bound and ligand-free conformations as it moves 11.2 Å inward to form a hydrogen bond (2.9 Å) with the side chain of Y261 (**Figure 2.1A**), creating a gate that seals the active site upon NAD$^+$ binding (**Figure 2.1B**).[5, 29, 35] Given the distal position of the αC atom of Q80 from the N$_5$ atom of the FMN (15.4 Å; **Figure 2.1C**), we propose that mutation of Q80 will not have a detrimental effect on NQO catalysis. However, as Q80 controls the opening and closing of the active site gate (**Figure 2.1D**), it may play a role in the substrate NADH binding in NQO.

The present study investigated the importance of Q80 in substrate binding in the active site of NQO by mutating Q80 to glycine, leucine, or glutamate. We have used site-directed mutagenesis, rapid kinetics, steady-state kinetics, and UV-visible absorption spectroscopy of Q80G, Q80L, and Q80E enzymes to understand the mechanistic role played by gating residue Q80 in substrate binding and catalysis.

2.3   Materials and methods

2.3.1   Materials:

The enzymes DpnI, calf intestinal alkaline phosphatase, and T4 DNA ligase were purchased from New England Biolabs (Ipswich, MA); DNA polymerase (*Pfu*) was from Stratagene (La Jolla, CA), and oligonucleotides were from Sigma Genosys (The Woodlands, TX). *P. aeruginosa* PAO1 genomic DNA was a gift from Dr. Jim Spain, Georgia Institute of Technology, Atlanta, GA. *E.coli* strain Rosetta(DE3)pLysS and the pET20b(+) expression vector were from Novagen (Madison, WI). DH5α *E. coli* strain was purchased from Life Technologies, Inc.; the QIAprep spin miniprep kit, QIAquick PCR purification kit, and QIAquick, gel extraction kit, were from Qiagen (Valencia, CA). HiTrap chelating HP 5-ml affinity column was from GE Healthcare, and isopropyl 1-thio-D-galactopyranoside (IPTG) was from Promega (Madison, WI). All quinones were purchased from Sigma-Aldrich (St. Louis, MO). NADH and NADPH disodium salts were purchased from VWR (Radnor, PA). All other reagents were of the highest purity commercially available.

2.3.2   Site-directed mutagenesis and protein purification:

The genes of NQO mutants Q80G, Q80L, and Q80E were prepared using a pET20b(+) plasmid harboring the wild-type gene PA1024 as a template and mutagenic primers containing corresponding site mutations.[36] The mutant genes were sent to Psomagen, Inc. for sequencing after mutagenesis. Plasmids were purified using the QIAquick spin Miniprep kit.[37] The constructs containing correct mutations were transformed into chemically competent *E. coli* strain Rosetta (DE3)pLysS by heat shock for protein expression.[38] The expression and purification of NQO mutant enzymes Q80G, Q80L, and Q80E, followed the protocol used for the wild-type enzyme as

previously described.[20] SDS-PAGE was used to determine the purity of the enzymes (data not shown).[39]

2.3.3 UV-visible absorption spectroscopy and extinction coefficient determination:

An Agilent Technologies diode-array spectrophotometer model HP 8453 PC (Santa Clara, CA), thermostated with a water bath, was used to record the UV-visible absorbance in 10 mM Tris-Cl, 200 mM NaCl, 10% glycerol, pH 8.0, at 25 °C. The extinction coefficients of the purified NQO wild-type and mutant enzymes were determined via heat denaturation by extracting the FMN cofactor from the enzymes.[40] The enzymes were passed through a PD-10 desalting column before heat denaturation at 100 °C for 20, 30, or 40 minutes.[41] Denatured protein was removed by centrifugation at 20,000×g. The concentration of the released FMN was determined spectroscopically by using ε_{450} of 12,200 M^{-1}cm^{-1} for free FMN.[20] The total protein concentration was determined using the Bradford method with bovine serum albumin as standard.[42]

2.3.4   Reductive half-reaction:

The anaerobic reduction of the enzyme-bound FMN with NADH in 20 mM KPi, 200 mM NaCl, and pH 7.0 was followed with an SF-61DX2 Hi-Tech KinetAssyst high-performance stopped-flow spectrophotometer (Bradford-on-Avon, UK), thermostated with a water bath at 25 °C. Anaerobiosis of the instrument and all buffers, substrates, and enzyme solutions was performed according to standard procedure.[20] NADH concentration was determined spectrophotometrically at 340 nm with an extinction coefficient at 6,220 M^{-1}cm^{-1}.[20] After mixing, the enzyme concentration was ~6 µM and NADH ranged from 60 to 500 µM to maintain pseudo-first-order conditions.

2.3.5 Apparent steady-state kinetics:

The turnover of NQO-Q80 mutant and NQO-WT enzymes with varying quinones (toluquinone, juglone, and CoQo) and fixed 100 µM NADH was monitored in 20 mM Kpi, 200 mM NaCl, pH 7.0, at 25 °C. The stock solutions of quinones were prepared in 100 % ethanol. The final ethanol concentration in all reaction mixtures was kept at 1% to minimize any possible effects of this solvent on enzymatic activity. The reaction rates were measured by following the NADH consumption at 340 nm, using ε_{340} of 6,220 M^{-1}cm^{-1}.[20]

2.3.6 Steady-state kinetics:

The steady-state kinetic mechanism of NQO-WT and NQO-mutants were determined at varying concentrations of NADH and 1,4-benzoquinone. The concentration range for NADH was 10-250 µM with mutant enzymes Q80G and Q80E and 5-200 µM with both NQO-WT and Q80L enzymes. The concentration of 1,4-benzoquinone was 10-200 µM with NQO-WT, 5-100 µM with Q80E and Q80L, and 10-250 µM with Q80G. The assays followed the initial reaction rates for each enzyme in 20 mM Kpi, 200 mM NaCl, pH 7.0, 25 °C.

2.3.7 Oxygen reactivity:

NADH oxidase activity was monitored on an Oxy-32 oxygen-monitoring system at atmospheric oxygen in 20 mM Kpi, 200 mM NaCl, pH 7.0, at 25 °C, following the initial rate of oxygen consumption, with a final NADH concentration of 400 µM.

2.3.8 Data analysis:

The apparent steady-state kinetic parameters at varying concentrations of NADH and fixed concentrations of quinones were determined by fitting the initial reaction rates to the Michaelis-Menten equation (eq 1). The steady-state kinetic parameters for the enzymatic assay were obtained by fitting the experimental points to the Michaelis-Menten equation using KaleidaGraph software

(Synergy Software, Reading, PA). The double reciprocal plot was constructed using KaleidaGraph, and global analysis was carried out using EnzFitter software (Biosoft, Cambridge, UK). The best fit of the initial reaction rate (v_o/e) was obtained with eq 2, which describes a ping-pong bi-bi steady-state kinetic mechanism.

$$v_o/\text{e} = \frac{k_{cat}\,[\text{A}]}{K_m + [\text{A}]} \qquad \text{(eq 1)}$$

$$v_o/\text{e} = \frac{k_{cat}\,AB}{K_a B + K_b A + AB} \qquad \text{(eq 2)}$$

In the above equation, v_o is the initial velocity, e represents the enzyme concentration, K_a and K_b are Michaelis constants for NADH (A) and 1,4-benzoquinone (B), and k_{cat} is the turnover rate at saturating concentration of both substrates.

Stopped-flow traces obtained with the KinetAsyst 3 (TgK-Scientific, Bradford on-Avon, UK) software were fit to eq 3, which describes a double-exponential process.

$$\text{A} = B_1{}^{-k_{obs1}t} + B_2{}^{-k_{obs2}t} + \text{C} \qquad \text{(eq 3)}$$

In this equation, A is the absorbance at 460 nm at time t; B_1 and B_2 are the amplitudes of the decrease in absorbance; k_{obs1} and k_{obs2} are the observed rate constants for the change in absorbance. C is an offset value accounting for the non-zero absorbance of the enzyme-bound reduced flavin at infinite time.

The concentration dependence for the observed rate constants of flavin reduction was analyzed with eq 4 where S represents the concentration of NADH, k_{red} is the rate of flavin reduction at saturating concentration of NADH, and K_d is the dissociation constant for NADH binding.

$$K_{obs} = \frac{k_{red}\, S}{K_d + S} \qquad\qquad (eq\ 4)$$

2.4   Results

2.4.1 Purification and spectral properties:

The NQO-Q80G, Q80L, and Q80E enzymes were purified to high levels following the same protocol previously used for the wild-type enzyme.[20] The presence of 200 mM NaCl in a storage buffer composed of 10 mM Tris-Cl, pH 8.0, and 10% glycerol was necessary for the *in vitro* stability of purified NQO enzymes.[20]
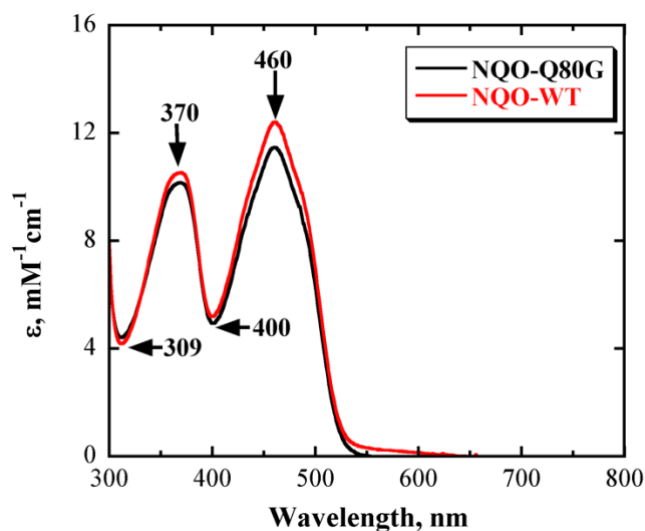
Figure 2.2: UV-visible absorption spectra of NQO-WT (solid red curve) and NQO-mutant Q80G (solid black curve). The UV-visible absorption spectra were recorded in 10 mM Tris-Cl, 200 mM NaCl, 10% v/v glycerol, at pH 8.0 and 25 °C.

The spectroscopic properties of the mutant enzymes were analyzed using UV-visible absorption spectroscopy to evaluate whether the mutation had an effect on the active site microenvironment in NQO. The UV-visible absorption spectrum of the purified mutant enzymes Q80G (**Figure 2.2**), Q80L (data not shown), and Q80E (data not shown) showed maximal absorbance at 370 nm and 460 nm, which is consistent with the presence of an FMN cofactor. All variant enzymes showed minimal difference in the absorption wavelength at 460 nm and 370 nm

compared to the wild-type enzyme (**Table 2.1**).[40] The FMN to protein stoichiometry was ~0.4 for

all mutants, similar to the stoichiometry determined for the wild-type enzyme (**Table 2.1**).

Table 2.1: UV-visible absorption maxima and FMN/protein stoichiometry of wild type and mutated NQO

Enzymes	$^a\lambda_{peaks}$, nm	$^b\varepsilon$, mM^{-1}cm^{-1}		FMN/Protein
		370	**460**	
WT	370, 460	10.6	12.2	0.40
Q80G	370, 460	10.0	11.2	0.35
Q80L	370, 460	10.2	11.4	0.33
Q80E	370, 460	10.5	12.5	0.41

^{a}Spectra were recorded in 10 mM Tris-Cl, 200 mM NaCl, 10% v/v glycerol, pH 8, 25 °C. ^{b}Molar extinction coefficient. Standard errors were ≤10%.

2.4.2 Steady-state kinetics:

The steady-state kinetic parameters of the NQO-Q80G, Q80L, and Q80E enzymes were

determined and compared to those of NQO-WT to investigate how the mutation of the gating

residue Q80 affects the rate of substrate capture and turnover of NQO. The steady-state kinetic

parameters were determined by the rate of NADH consumption at varying concentrations of both

NADH and 1,4-benzoquinone (BQ) at pH 7.0 and 25 °C. The best fits for the kinetic parameters

of the NQO-mutant and wild-type enzymes were obtained using an equation describing a ping-

pong bi-bi steady-state mechanism (eq 2). The data suggest that the Q80 mutations did not alter

the mechanism (ping-pong bi-bi) NQO utilizes in its catalytic turnover (**Figure 2.3**). With all

variant enzymes, the k_{cat} values differed from the wild-type NQO by <1.5-fold (Table 2). The

k_{cat}/K_{NADH} value decreased 5-fold for the Q80G enzyme and only <2.5-fold for both Q80L and

Q80E enzymes compared to the wild-type NQO. However, the k_{cat}/K_{BQ} for Q80G, Q80L, and

Q80E enzymes were similar to the NQO wild type enzyme (**Table 2.2**).
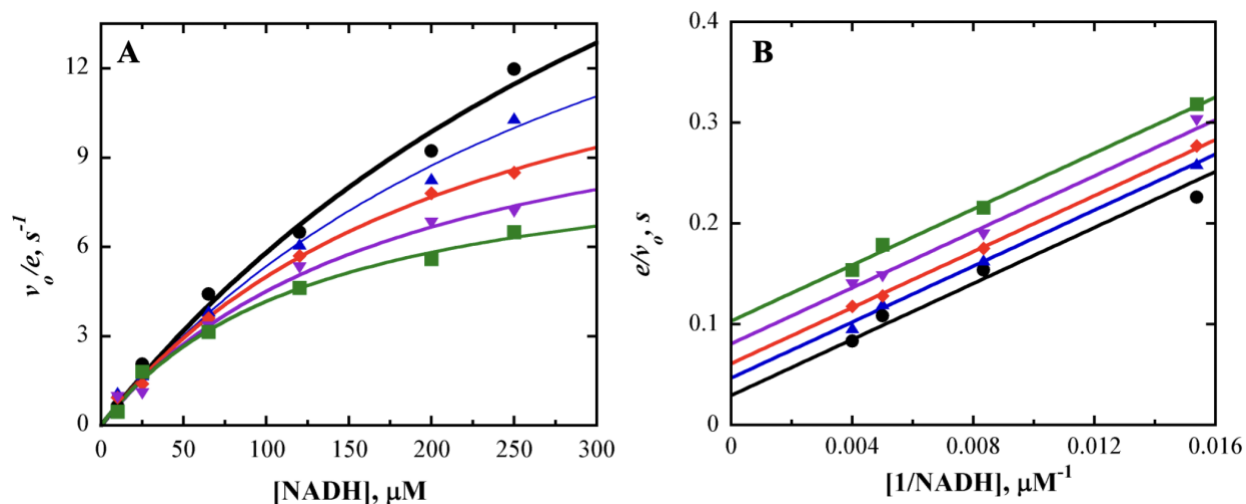
Figure 2.3: Steady-state kinetics of NQO-Q80G with NADH and 1,4-benzoquinone as substrates. (A) Michaelis-Menten plot; (B) Lineweaver- Burk plot. The initial rate of reaction was measured at varying NADH (10 µM to 250 µM) and 1,4-benzoquinone (BQ) (5 µM to 100 µM) concentrations in 20 mM Kpi, 200 mM NaCl, pH 7.0, 25 $^{\circ}$C. Green = 5 µM BQ, Purple = 10 µM BQ, Red = 25 µM BQ, Blue = 50 µM BQ, and Black = 100 µM BQ. Data were fitted to eq 2.

Table 2.2: ^{a}Steady-state kinetic parameters of NQO-WT, NQO-Q80G, NQO-Q80L, and NQO-Q80E with NADH and 1,4-benzoquinone as substrates

Enzyme	k_{cat}, s^{-1}	k_{cat}/K_{NADH}, M^{-1}s^{-1}	k_{cat}/K_{BQ}, M^{-1}s^{-1}	K_{NADH}, µM	K_{BQ}, µM
WT	27	400,000	930,000	70	30
Q80G	27	75,000	1,400,000	360	20
Q80L	23	120,000	800,000	180	30
Q80E	20	200,000	1,400,000	120	15

^{a}Enzymatic activity was measured by varying concentrations of both NADH and 1,4-Benzoquinone in 20 mM KPi, 200 mM NaCl, pH 7.0, 25°C. Steady-state kinetic parameters were measured following NADH reduction using the extinction coefficient for NADH at $\varepsilon_{340} = 6,220$ M^{-1}cm^{-1}. Standard errors were ≤17%.

2.4.3   Reductive half-reaction:

The reductive-half reaction of the NQO-Q80G, Q80L, and Q80E enzymes was investigated at pH 7.0 and 25 °C by monitoring the decrease in absorbance at 460 nm as a measure of the rate of flavin reduction using a stopped-flow spectrophotometer. The mutant enzymes were fully reduced with NADH in a biphasic pattern (**Figure 2.4A**). The fast phase accounted for more than 95% of the total absorbance change at 460 nm and was attributed to flavin reduction. The slow phase, accounting for less than 5% of the complete change of absorbance at 460 nm, was attributed to the damaged enzyme and had a k_{obs} value of ~1 s^{-1} independent of substrate concentration. The data obtained from flavin reduction were analyzed with eq 3, revealing that the mutant enzyme NQO-Q80G was thoroughly saturated with NADH at 200 µM. For the Q80E and Q80L enzymes, NADH was saturating at 100 µM. A plot of the k_{obs} values as a function of NADH concentration yielded a concentration-dependent hyperbolic curve (**Figure 2.4B**), which determined the limiting rate constant for flavin reduction k_{red} for NQO-Q80 enzymes (**Table 2.3**). The dissociation constant for substrate binding (K_d) values were estimated for Q80G, Q80E, and Q80L enzymes (**Table 2.3**).

Table 2.3: [a]Reductive half-reaction of NQO-WT, NQO-Q80G, NQO-Q80L, and NQO-Q80E with NADH

Enzyme	k_{red} (s^{-1})	K_d (µM)
WT	25	≤ 3
Q80G	26	183
Q80L	27	80
Q80E	21	87

[a]The kinetic parameters were determined with (60-500 µM) NADH in 20 mM KPi, 200 mM NaCl, pH 7.0 at 25 °C. Standard errors were $\leq 30\%$.
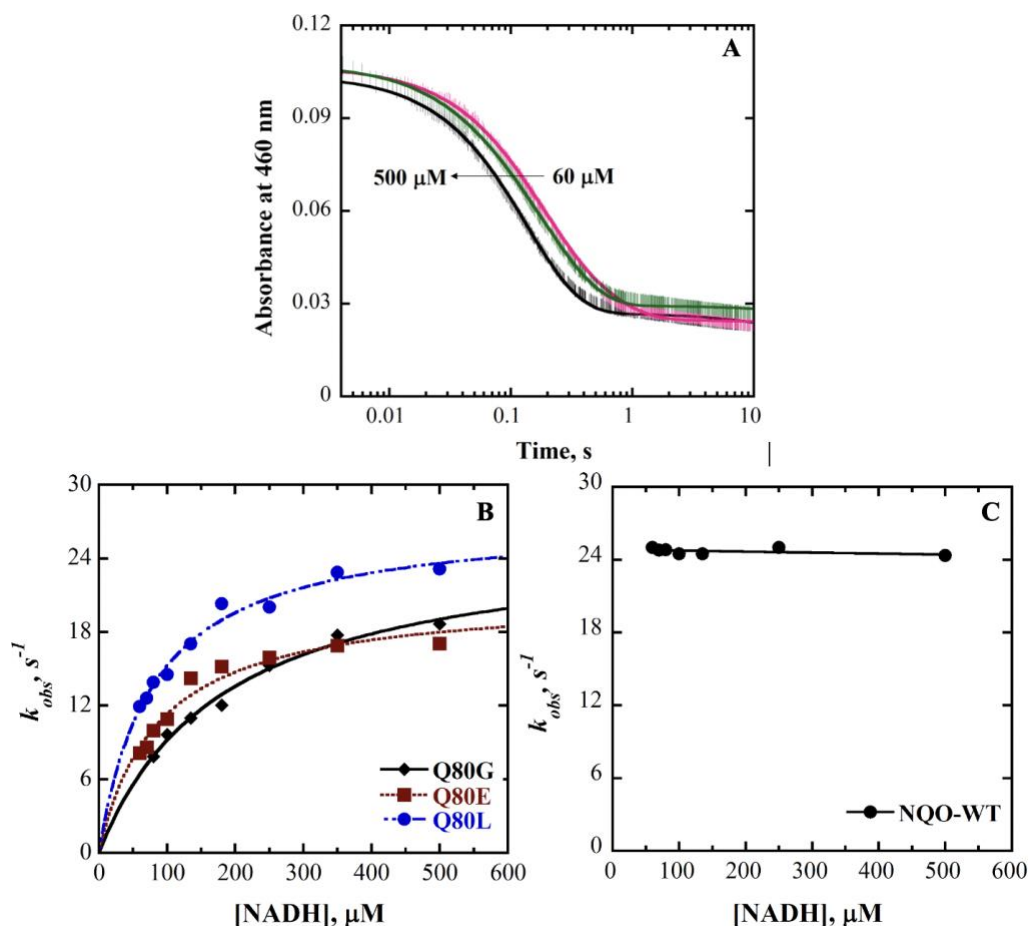
Figure 2.4: Anaerobic reduction of NQO-Q80 mutants and WT with NADH. (A) Stopped-flow traces of NQO-Q80G at 460 nm with varying concentrations of NADH (60-500 μM) fit eq 3. Note the log time scale. For clarity, one of the ten experimental points is shown (vertical lines). The instrumental dead time is 2.2 ms. (B) Concentration dependence of the observed rate constant (k_{obs}) for flavin reduction of Q80G (black), Q80E (maroon), and Q8OL (blue) with NADH. (C) Concentration dependence of the k_{obs} value for flavin reduction of NQO-WT with NADH. The solid curve was generated by fitting the data to eq 4. Activity assays were performed in 20 mM KPi, and 200 mM NaCl at pH 7.0 and 25 °C.

An accurate K_d value was not determined for the wild type enzyme as it was not possible to lower the NADH concentration below 60 μM to maintain pseudo-first-order conditions. However, the observation that the NQO-WT was thoroughly saturated with 60 μM NADH (**Figure 2.4C**) suggests a K_d value might be around 3 μM. Assuming there is ~5 to 10% inherent error in

the estimated k_{obs} value at 60 µM NADH, a K_d value of 3 to 5 µM can be calculated using equation 4. The K_d value for the Q80G enzyme increases by ≥60-fold, and those of Q80L and Q80E enzymes increase by ≥30-fold (**Table 2.3**) compared to wild-type NQO. When the enzymes were anaerobically mixed with 500 µM NADPH, the enzyme-bound flavin was slowly reduced (~10% over 10 min) with Q80G (**Figure 2.5**), Q80L, Q80E, and wild-type NQO (data not shown), consistent with NQO enzymes were not reactive with NADPH.
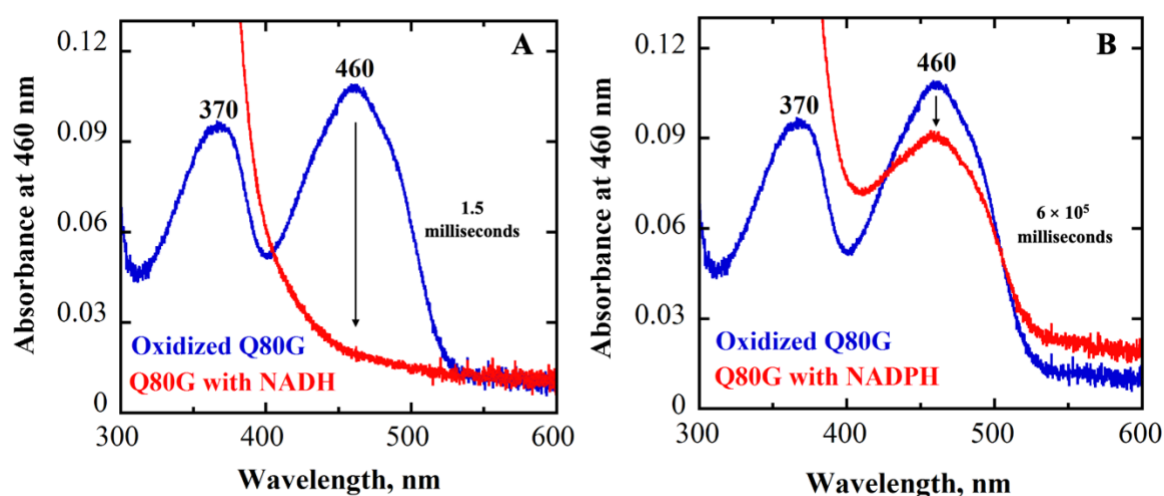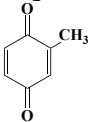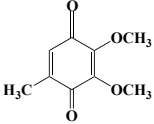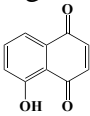
Figure 2.5: Reduction of NQO-Q80G with NADH (A) and NADPH (B). The time-resolved absorption spectra were observed at 8 µM Q80G mixed with 60 µM NADH and 500 µM NADPH at pH 7 and 25 °C. Blue lines represent the spectra of oxidized flavin bound to Q80G. The red line of each plot corresponds to the spectrum of flavin hydroquinone recorded after 1.5 ms with NADH (A) and 10 mins with NADPH (B). The arrows represent the degree of flavin reduction, ~90 % in A and ~10 % in B.

2.4.4   Enzyme activity with oxidizing substrates:

The NQO from *P. aeruginosa* was previously established to be active with quinones.[19] To evaluate whether the Q80 in loop 3 of NQO has a role in substrate quinone binding, the enzymatic turnover of NQO-Q80 enzymes was determined with different quinones. The activity of NQO-Q80 enzymes was measured with the methods of initial rates using either toluquinone, 2,3-

dimethoxy 5-methyl 1,4-benzoquinone (CoQo), or 5-hydroxy 1,4-naphthoquinone (juglone), as substrate with fixed 100 µM NADH concentration at pH 7.0 and 25 °C. The k_{cat}/K_m values determined at a sub-saturating concentration of NADH reflect the true k_{cat}/K_m values since NQO follows ping-pong bi-bi steady-state kinetics,[57,] which is characterized by unchanging k_{cat}/K_m values despite the concentration of the fixed substrate. As shown in Table 2.4, the NQO-Q80 mutants have a negligible impact on the kinetic parameter k_{cat}/K_m compared to the wild-type NQO.

Table 2.4: Apparent steady-state kinetics of NQO-WT, Q80G, Q80L, and Q80E enzymes with varying quinones and fixed NADH concentration

Enzyme	Quinone	k_{cat}/k_m, M^{-1}s^{-1}
WT	Toluquinone	290,000
Q80G		300,000
Q80L		210,000
Q80E		350,000
WT	CoQo	300,000
Q80G		280,000
Q80L		250,000
Q80E		400,000
WT	Juglone	720,000
Q80G		540,000
Q80L		820,000
Q80E		790,000

[a]The kinetic parameters were determined with 100 µM NADH in 20 mM KPi, 200 mM NaCl, pH 7.0 at 25 °C. The kinetic parameter k_{cat} was between 15-25 s^{-1}, and K_m was between 10-100 µM. Standard errors were ≤ 25%.

2.4.5 NADH oxidase activity:

The activity of the NQO mutants with molecular oxygen as an electron acceptor was investigated with 20-400 µM NADH using Clark-type oxygen electrode. There was no significant oxygen consumption with the NQO mutant and NQO-WT enzymes. The average oxygen consumption rate for the NQO-mutants was <1 s^{-1}, which is lower than the oxidase activity

observed for the WT enzyme with NADH ($\sim$3 s^{-1}) under the same conditions. However, after adding 1 mM PMS (artificial electron acceptor) to regenerate the oxidized enzyme in the reaction mixture, there was a rapid oxygen depletion, which indicates that the enzymes were active (data not shown).[46]

2.5   Discussion

A comparison of the previously solved crystal structures of ligand-bound and ligand-free NQO indicates that a conformational change occurs at loop 3 (residues 75-86).[29] Q80 in loop 3 switches between an open conformation without NAD$^+$ bound and a close conformation with NAD$^+$ bound.[29] Q80 acts as a gate that interacts with Y261 to secure NAD$^+$ within the binding pocket of NQO.[29] In addition, the backbone amide of Q80 (3.4 Å) forms a hydrogen bond with the O1 and O2 atoms of the adenine phosphate of NAD$^+$.[29] In the present study, substituting Q80 with glycine, leucine, or glutamate through site-directed mutagenesis revealed that Q80 is important for NADH binding. The rapid and steady-state kinetics presented here demonstrate that the binding affinity of NQO for NADH was significantly decreased in the Q80 mutant enzymes compared to NQO-WT; however, the mutations did not affect the rate of hydride transfer. Furthermore, NQO did not acquire a new activity for NADPH when the bulky Q80 sidechain was entirely removed. These conclusions are supported by the evidence provided below.

Glutamine 80 is important for NADH binding in NQO. Evidence to support this conclusion comes from the reductive half-reaction of the NQO mutants and NQO-WT with NADH at pH 7.0 and 25 °C. The wild type enzyme has a dissociation constant for substrate binding (K_d) of ≤ 3 µM (**Table 2.3**). The K_d value increases $\sim$60-fold in the Q80G enzyme and $\sim$30-fold in both the Q80L and Q80E enzymes (**Table 2.3**). The crystal structure of NQO with bound NAD$^+$ reveals that Q80 forms a hydrogen-bond with Y261, which seals the active site gate to secure NADH (Figure 1

B).[29] The mutation of Q80 to glycine creates a more open active site entrance as glycine has no side chain, which decreases the affinity of NQO for NADH. On the other hand, leucine and glutamate have a similar side chain size as glutamine, making the binding affinity of Q80L and Q80E enzymes for NADH better than the Q80G enzyme. Furthermore, leucine is nonpolar and has no propensities for a hydrogen-bond interaction with Y261. The open conformation of the NQO-WT crystal structure reveals a possible hydrogen-bond interaction between Q80 and proline 78 (3 Å). Since glutamate has a charge, there might be a possibility of a tighter binding of E80 with P78 and less interaction with Y261. Therefore, the closed conformation of both Q80L and Q80E enzymes will be less favored, resulting in a lower binding affinity of Q80L and Q80E enzymes for NADH than the wild-type enzyme.

Q80 does not participate in the hydride transfer reaction from NADH to the NQO enzyme-bound flavin. Evidence to support this conclusion comes from the reductive half-reaction of NQO mutants and the NQO-WT enzyme with NADH as a substrate. The hydride transfer rate was similar in NQO enzymes regardless of the residue at position 80. Since the αC of Q80 is 15.4 Å away from the N_5 atom of the FMN cofactor; [29] therefore, the alteration of distal gating Q80 residue in loop 3 would have little to no effect on NQO catalysis. Gating residues and loops are attractive targets for protein engineering since they are the natural site for mutations during protein evolution.[1,5, 12-15] Moreover, modulation of the gating residue is not detrimental to protein function since the residue is often spatially separated from the active site of the enzyme.[16-18] Therefore, the data in our study agreed with the expectations for gating residues as promising targets for protein engineering, since the mutation of gating Q80 residue mediates the rate of NADH binding without affecting the rate of hydride transfer from NADH to the enzyme bound flavin. Interestingly, a study on dihydrofolate reductase from *E. coli* reported that mutation of glycine 121(G121), which

is 19 Å away from the catalytic center, did not only decrease the binding of the NADPH substrate (~40-fold) but also decreased the rate of hydride transfer by ~200- fold.[47] The change of G121 would alter this residue's dynamic feature, which causes the conformational changes of mutant enzymes preceding hydride transfer.[44] However, the analysis of the previous study suggests that the replacement of Q80 with G, L, or E would not probably alter the dynamic feature of this residue proceeding for hydride transfer; it instead alters the access of NADH in the active site of the enzyme.

Q80 has no role in the specificity constant of NQO for substrate quinones. Evidence to support this conclusion comes from the apparent steady-state and steady-state kinetics of NQO-WT and mutants with NADH and quinones (1,4-benzoquinone, juglone, CoQo, and toluquinone) (**Tables 2.2 & 2.4**). The k_{cat}/K_m value measures the rate of capture of the substrate into an enzyme-substrate complex that proceeds to catalysis and is therefore used to report the specificity constant of the enzyme for a substrate.[45-50] The quinones had similar k_{cat}/K_m values across NQO mutants and NQO-WT, suggesting that Q80 mutation had a negligible impact on the capture of the substrate quinones. The trend is different from the substrate NADH, where the k_{cat}/K_m values change (2-5-fold) across the mutations. However, the degree of change in k_{cat}/K_m values with NADH was not similar to k_{red}/K_d (~30-60-fold change) in NQO enzymes. Since the NQO-WT enzyme undergoes an internal isomerization from the ES complex to form an ES*,[52] the additional step in the enzyme catalytic pathway might impact the k_{cat}/K_m values of NQO for NADH. However, NADH is a bulkier substrate than quinones, whose ribose, pyrophosphate, and adenine moieties interact with residues adjacent to the gate region of NQO. Given these structural differences, the quinones would have easier access and mobility to and from the active site of NQO. Therefore, there might

be no changes in the mobility and catalysis of the quinones with the Q80G, Q80L, and Q80E enzymes as the active site gate remain broad enough for a quinone capture.

The rate of NADH dissociation from the ES complex is faster than the chemical step of catalysis in NQO-Q80G, Q80L, and Q80E enzymes. Evidence to support this conclusion comes from the reductive half-reaction and steady-state kinetics of NQO mutants and NQO-WT with NADH, which measure the K_d and K_m values, respectively. The K_d is the ratio of the reverse and forward rate constants for substrate binding[58,59] and is different from the K_m in that K_m includes the chemical step of catalysis (k_3).[58,60] The K_m and K_d are equal when the k_3 is much slower than the rate of substrate dissociation (k_2) from the ES complex.[58] In NQO-WT, the $K_{d(NADH)}$ value is 25-fold lower than the $K_{m(NADH)}$ value. Since Q80 keeps NADH tightly bound in the binding pocket of NQO, the rate of hydride transfer from NADH to the NQO-bound flavin might be faster than the rate of substrate NADH dissociation from ES complex or the rate of product NAD^+ released from EP complex. On the other hand, the NQO-Q80G, Q80L, and Q80E enzymes have similar $K_{m(NADH)}$ and $K_{d(NADH)}$ values (overall 1-2.5-fold difference), suggesting that the rate of chemical step in the NQO mutants might be much slower than NADH dissociation. The Q80G enzyme prevents all potential interactions by increasing the space around the active site gate, which most likely causes a rapid rate of NADH dissociation. The replacement of Q80 with nonpolar leucine has no key interaction for substrate NADH binding, which might enhance NADH dissociation. The negative charge E80 in NQO-Q80E might have an electrostatic repulsion with two phosphate groups of NADH, which would also increase NADH dissociation.

Flavin reduction is fully rate-limiting in the NQO mutants and wild type enzyme. Evidence to support this conclusion comes from the reductive half-reaction with NADH and the steady-state kinetics with NADH and 1,4-benzoquinone for NQO mutants and NQO-WT. The k_{cat} and k_{red}

values were 5% similar for NQO-WT and Q80G and Q80E enzymes and 17% similar for Q80L

enzyme (**Table 2.2 & 2.3**). The k_{cat} of a reaction is determined by the turnover rate of the enzyme

at saturating concentration of substrates; it may or may not include the chemical step and is often

limited by the actual release of a product.[54, 55, 60] Since the k_{cat} and k_{red} values were similar, k_{red} is

the limiting step of catalysis in NQO and fully rate-limiting for catalytic turnover. Therefore, the

product release is fast in all NQO enzymes, regardless of the residue at position 80. Given the

crystal structures of the ligand-bound and free forms of NQO[29] (**Figure 2.1**), the Q80-Y261

hydrogen bond dissociates after NADH oxidation and loop 3 to swing outward (5.5Å) in the open

conformation for product release. With this loop motion and open active site gate, the residue at

position 80 should not impact the rate of product release. Since the rate of product release will be

fast for both the NQO mutant and NQO-WT, the k_{cat} will be dictated by the k_{red} of the reaction.

The NQO-Q80G, Q80L, and Q80E enzymes did not acquire the ability to use NADPH as

a reducing substrate. Evidence to support this conclusion comes from the reductive half-reaction

of NQO-Q80 mutants with NADPH at pH 7.0 at 25 °C (**Figure 2.5**). The NQO mutants showed a

higher preference for NADH over NADPH. The flavin reduction of NQO-Q80G, Q80L, and Q80E

enzymes was 90% over 1.5 milliseconds with 500 µM NADH (**Figure 2.5A**). In contrast, the

enzyme bound flavin was not significantly reduced (10% over 10 min) with the equivalent

concentration of NADPH in NQO mutant enzymes (**Figure 2.5B**). Therefore, Q80 of NQO has no

role in obtaining the reactivity for NADPH. In a previous study, the homology modeling and

docking analysis of the bifunctional alcohol/aldehyde dehydrogenase from *Clostridium*

thermocellum with NADPH suggested that the extra phosphate of NADPH would encounter

electrostatic repulsion and steric hindrance with D494. [36] Therefore, the mutation of D494 with

glycine increased the specificity of NADPH in *C. thermocellum* bifunctional alcohol/aldehyde

dehydrogenase.[36] From the analysis of the previous study, it was expected that the replacement of Q80 with glycine would decrease the steric clashes with NADPH and increase the reactivity of NQO for NADPH. However, the data from our study suggests otherwise. The decrease in the specificity of NQO for NADPH in all the variant enzymes suggests that Q80 has no significant impact on the reactivity of NQO with NADPH.

In summary, the results presented in this study demonstrate that the glutamine 80 in loop 3 plays a vital role in controlling NADH binding in NQO without impacting the hydride transfer from NADH to flavin. The replacement of bulky Q80 residue of NQO with glycine results in a more open active site gate that lowers the binding affinity of NQO-Q80G for NADH. On the other hand, mutation of Q80 to a residue of a similar sidechain length (~4 Å), either nonpolar or charged, such as leucine (L) or glutamate (E), respectively, also lowers the binding affinity of Q80L and Q80E enzymes for NADH. However, the Q80 mutant enzymes did not impact the rate of substrate quinones capture. Regardless of the residue at position 80 of NQO, the rate-limiting step of the enzymes was unchanged, with no observed increase in NADPH reactivity. The data presented in our study agreed with the expectations for gating residues as promising targets for protein engineering. Since the mutation of gating Q80 residue mediates the rate of NADH affinity without affecting the hydride transfer rate.

2.6 References:

[1] Gora, A., Brezovsky, J., and Damborsky, J. (2013) Gates of Enzymes, *Chem. Rev. 113*, 5871-5923.

[2] Cui, Q., and Karplus, M. (2008) Allostery and cooperativity revisited, *Protein Sci. 17*, 1295-1307.

[3] Couture, J.-F., Legrand, P., Cantin, L., Labrie, F., Luu-The, V., and Breton, R. (2004) Loop Relaxation, A Mechanism that Explains the Reduced Specificity of Rabbit 20α-Hydroxysteroid Dehydrogenase, A Member of the Aldo-Keto Reductase Superfamily, *J. Mol. Biol 339*, 89-102.

[4] Marques, S. M., Daniel, L., Buryska, T., Prokop, Z., Brezovsky, J., and Damborsky, J. (2017) Enzyme Tunnels and Gates As Relevant Targets in Drug Design, *Med. Res. Rev. 37*, 1095-1139.

[5] Nestl, B. M., and Hauer, B. (2014) Engineering of Flexible Loops in Enzymes, *ACS Catal. 4*, 3201-3211.

[6] Nussinov, R., and Tsai, C.-J. (2013) Allostery in Disease and in Drug Discovery, *Cell 153*, 293-305.

[7] Papaleo, E., Saladino, G., Lambrughi, M., Lindorff-Larsen, K., Gervasio, F. L., and Nussinov, R. (2016) The Role of Protein Loops and Linkers in Conformational Dynamics and Allostery, *Chem. Rev. 116*, 6391-6423.

[8] Pasi, M., Riccardi, L., Fantucci, P., De Gioia, L., and Papaleo, E. (2009) Dynamic properties of a psychrophilic α-amylase in comparison with a mesophilic homologue, *J. Phys. Chem. B 113*, 13585-13595.

[9] Fu, G., Yuan, H., Li, C., Lu, C.-D., Gadda, G., and Weber, I. T. (2010) Conformational changes and substrate recognition in *Pseudomonas aeruginosa* D-arginine dehydrogenase, *Biochemistry 49*, 8535-8545.

[10] Richard, J. P. (2019) Protein Flexibility and Stiffness Enable Efficient Enzymatic Catalysis, *J. Am. Chem. Soc. 141*, 3320-3331.

[11] Ouedraogo, D., Souffrant, M., Vasquez, S., Hamelberg, D., and Gadda, G. (2017) Importance of Loop L1 Dynamics for Substrate Capture and Catalysis in *Pseudomonas aeruginosa* d-Arginine Dehydrogenase, *Biochemistry 56*, 2477-2487.

[12] Gunasekaran, K., and Nussinov, R. (2004) Modulating Functional Loop Movements: The Role of Highly Conserved Residues in the Correlated Loop Motions, *Chem.Bio.Chem. 5*, 224-230.

[13] Gao, B., Xu, T., Lin, J., Zhang, L., Su, E., Jiang, Z., and Wei, D. (2011) Improving the catalytic activity of lipase LipK107 from Proteus sp. by site-directed mutagenesis in the lid domain based on computer simulation, *J. Mol. Catal. B: Enzym. 68*, 286-291.

[14] Coleman, C. S., Stanley, B. A., and Pegg, A. E. (1993) Effect of mutations at active site residues on the activity of ornithine decarboxylase and its inhibition by active site-directed irreversible inhibitors, *J. Biol. Chem. 268*, 24572-24579.

[15] Brouk, M., Derry, N.-L., Shainsky, J., Zelas, Z. B.-B., Boyko, Y., Dabush, K., and Fishman, A. (2010) The influence of key residues in the tunnel entrance and the active site on activity and selectivity of toluene-4-monooxygenase, *J. Mol. Catal. B: Enzym. 66*, 72-80.

[16] Inouye, M. (2016) The first application of site-directed mutagenesis using oligonucleotides for studying the function of a protein, *Gene 593*, 342-343.

[17] Thanki, N., Zeelen, J. P., Mathieu, M., Jaenicke, R., Abagyan, R. A., Wierenga, R. K., and Schliebs, W. (1997) Protein engineering with monomeric triosephosphate isomerase (monoTIM): the modelling and structure verification of a seven-residue loop, *Protein Eng. Des. Sel. 10*, 159-167.

[18] Yaacob, N., Ahmad Kamarudin, N. H., Leow, A. T. C., Salleh, A. B., Rahman, R. N. Z. R. A., and Ali, M. S. M. (2019) Effects of Lid 1 Mutagenesis on Lid Displacement, Catalytic Performances and Thermostability of Cold-active Pseudomonas AMS8 Lipase in Toluene, *Comput. Struct. Biotechnol. J. 17*, 215-228.

[19] Salvi, F., Rodriguez, I., Hamelberg, D., and Gadda, G. (2016) Role of F357 as an oxygen gate in the oxidative half-reaction of choline oxidase, *Biochemistry 55*, 1473-1484.

[20] Ball, J., Salvi, F., and Gadda, G. (2016) Functional annotation of a presumed nitronate monoxygenase reveals a new class of NADH: quinone reductases, *J. Biol. Chem. 291*, 21160-21170.

[21] Deller, S., Macheroux, P., and Sollner, S. (2008) Flavin-dependent quinone reductases, *Cell. mol. life sci. 65*, 141-160.

[22] Atia, A., Alrawaiq, N., and Abdullah, A. (2014) A review of NAD (P) H: Quinone oxidoreductase 1 (NQO1); A multifunctional antioxidant enzyme, *J. Appl. Pharm. Sci. 4*, 118-122.

[23] Brunmark, A., and Cadenas, E. (1989) Redox and addition chemistry of quinoid compounds and its biological implications, *Free Radic. Biol. Med. 7*, 435-477.

[24] Sollner, S., Nebauer, R., Ehammer, H., Prem, A., Deller, S., Palfey, B. A., Daum, G., and Macheroux, P. (2007) Lot6p from Saccharomyces cerevisiae is a FMN-dependent reductase with a potential role in quinone detoxification, *FEBS. J. 274*, 1328-1339.

[25] Deller, S., Macheroux, P., and Sollner, S. (2007) Flavin-dependent quinone reductases, *Cell. Mol. Life Sci. 65*, 141.

[26] Dratch, B. D., Orozco-Gonzalez, Y., Gadda, G., and Gozem, S. (2021) Ionic Atmosphere Effect on the Absorption Spectrum of a Flavoprotein: A Reminder to Consider Solution Ions, *J. Phy. Chem. Let. 12*, 8384-8396.

[27] Knox, R. J., Jenkins, T. C., Hobbs, S. M., Chen, S., Melton, R. G., and Burke, P. J. (2000) Bioactivation of 5-(aziridin-1-yl)-2, 4-dinitrobenzamide (CB 1954) by human NAD(P)H quinone oxidoreductase 2: a novel co-substrate-mediated antitumor prodrug therapy, *Cancer Res. 60*, 4179-4186.

[28] Sevostyanova, A., Belogurov, G. A., Mooney, R. A., Landick, R., and Artsimovitch, I. (2011) The β subunit gate loop is required for RNA polymerase modification by RfaH and NusG, *Mol. cell. 43*, 253-262.

[29] Ball, J., Reis, R. A., Agniswamy, J., Weber, I. T., and Gadda, G. (2019) Steric hindrance controls pyridine nucleotide specificity of a flavin-dependent NADH: quinone oxidoreductase, *Protein Sci. 28*, 167-175.

[30] Wierenga, R. (2001) The TIM-barrel fold: a versatile framework for efficient enzymes, *FEBS. J. 492*, 193-198.

[31] Höcker, B., Jürgens, C., Wilmanns, M., and Sterner, R. (2001) Stability, catalytic versatility and evolution of the (βα) 8-barrel fold, *Curr. opin. biotechnol. 12*, 376-381.

[32] Lockhart, Z., and Knipe, P. C. (2018) Conformationally Programmable Chiral Foldamers with Compact and Extended Domains Controlled by Monomer Structure, *Angew. Chem. 130*, 8614-8618.

[33] Van Nues, R. W., and Brown, J. D. (2004) Saccharomyces SRP RNA secondary structures: a conserved S-domain and extended Alu-domain, *RNA 10*, 75-89.

[34] Thanki, N., Zeelen, J. P., Mathieu, M., Jaenicke, R., Abagyan, R., Wierenga, R., and Schliebs, W. (1997) Protein engineering with monomeric triosephosphate isomerase (monoTIM): the modelling and structure verification of a seven-residue loop, *Protein eng. 10*, 159-167.

[35] Pettersen, E. F., Goddard, T. D., Huang, C. C., Couch, G. S., Greenblatt, D. M., Meng, E. C., and Ferrin, T. E. (2004) UCSF Chimera—a visualization system for exploratory research and analysis, *J. Comput. Chem. 25*, 1605-1612.

[36] Afonine, P. V., Grosse-Kunstleve, R. W., Echols, N., Headd, J. J., Moriarty, N. W., Mustyakimov, M., Terwilliger, T. C., Urzhumtsev, A., Zwart, P. H., and Adams, P. D. (2012) Towards automated crystallographic structure refinement with phenix.refine, *Acta. Cryst. D Biol. Cryst. 68*, 352-367.

[37] Steffens, D. L., and Williams, J. G. (2007) Efficient site-directed saturation mutagenesis using degenerate oligonucleotides, *J. Biomol. Tech. 18*, 147.

[38] Pronobis, M. I., Deuitch, N., and Peifer, M. (2016) The Miraprep: A protocol that uses a Miniprep kit and provides Maxiprep yields, *PLoS One 11*, e0160509.

[39] Inoue, H., Nojima, H., and Okayama, H. (1990) High efficiency transformation of Escherichia coli with plasmids, *Gene 96*, 23-28.

[40] Fujita, T., Shiota, K., Yoshikawa, J., Ogawa, S., and Aoyagi, H. (2019) Simple method for analyzing the purity of protease-containing samples by acid-treatment SDS-PAGE, *J. Biosci. Bioeng. 128*, 630-635.

[41] Hayes, W. A., Mills, D. S., Neville, R. F., Kiddie, J., and Collins, L. M. (2011) Determination of the molar extinction coefficient for the ferric reducing/antioxidant power assay, *Anal. Biochem. 416*, 202-205.

[42] Kim, H.-S., and Huber, K. C. (2007) Simple purification (desalting) procedure to facilitate structural analysis of an alkali-solubilized/neutralized starch solution by intermediate-pressure size-exclusion chromatography, *J. Agric. Food Chem. 55*, 4944-4948.

[43] Kruger, N. J. (2009) The Bradford method for protein quantitation, *Protein Protocol Handbook*, 17-24.

[44] Quaye, J. A., and Gadda, G. (2020) Kinetic and Bioinformatic Characterization of d-2-Hydroxyglutarate Dehydrogenase from *Pseudomonas aeruginosa* PAO1, *Biochemistry 59*, 4833-4844.

[45] Cameron, C. E., and Benkovic, S. J. (1997) Evidence for a functional role of the dynamics of glycine-121 of Escherichia coli dihydrofolate reductase obtained from kinetic analysis of a site-directed mutant, *Biochemistry 36*, 15792-15800.

[46] Stenberg, G., Board, P., Carlberg, I., and Mannervik, B. (1991) Effects of directed mutagenesis on conserved arginine residues in a human class alpha glutathione transferase, *Biochem. J. 274*, 549-555.

[47] Chen, K., Robinson, A. C., Van Dam, M. E., Martinez, P., Economou, C., and Arnold, F. H. (1991) Enzyme engineering for nonaqueous solvents. II. Additive effects of mutations on the stability and activity of subtilisin E in polar organic media, *Biotechnol. Prog. 7*, 125-129.

[48] Huang, L., Ma, H. M., Yu, H. L., and Xu, J. H. (2014) Altering the substrate specificity of reductase CgKR1 from Candida glabrata by protein engineering for bioreduction of aromatic α-keto esters, *Adv. Synt. Catal. 356*, 1943-1948.

[49] Meng, X., Yang, L., Liu, Y., Wang, H., Shen, Y., and Wei, D. (2021) Identification and Rational Engineering of a High Substrate-Tolerant Leucine Dehydrogenase Effective for the Synthesis of L-tert-Leucine, *Chem. Cat. Chem. 13*, 3340-3349.

[50] Roberge, M., Shareck, F., Morosoli, R., Kluepfel, D., and Dupont, C. (1998) Site-directed mutagenesis study of a conserved residue in family 10 glycanases: histidine 86 of xylanase A from Streptomyces lividans, *Protein Eng. 11*, 399-404.

[51] Wongsantichon, J., Harnnoi, T., and Ketterman, A. J. (2003) A sensitive core region in the structure of glutathione S-transferases, *Biochem. J. 373*, 759-765.

[52] [Quaye, J. A., Ball, J., and Gadda, G. (2022) Kinetic solvent viscosity effects uncover an internal isomerization of the enzyme-substrate complex in Pseudomonas aeruginosa PAO1 NADH: Quinone oxidoreductase, *Arch. Biochem. Biophys. 727*, 109342.

[53] Cohlberg, J. A. (1979) Km as an apparent dissociation constant, *J. Chem. Educ. 56*, 512.

[54] Nazzal, G. (2016) The relative values of the turnover number and the dissociation rate constant determine the definition of the Michaelis-constant, *bioRxiv*, 052514.

[55] Maenpuen, S., Watthaisong, P., Supon, P., Sucharitakul, J., Parsonage, D., Karplus, P. A., Claiborne, A., and Chaiyen, P. (2015) Kinetic mechanism of l–α–glycerophosphate oxidase from Mycoplasma pneumoniae, *Fed. Europ. Biochem. Soc. J. 282*, 3043-3059.

[56] Pollegioni, L., Langkau, B., Tischer, W., Ghisla, S., and Pilone, M. S. (1993) Kinetic mechanism of D-amino acid oxidases from Rhodotorula gracilis and Trigonopsis variabilis, *J. Biol.l Chem. 268*, 13850-13857.

[57] Mitchell, D. A., and Krieger, N. (2022) Looking through a new lens: Expressing the Ping Pong bi bi equation in terms of specificity constants, *Biochem. Eng. J. 178*, 108276.

[58] Cohlberg, J. A. (1979) Km as an apparent dissociation constant, *J. Chem. Educ. 56*, 512.

[59] Strickland, S., Palmer, G., and Massey, V. (1975) Determination of dissociation constants and specific rate constants of enzyme-substrate (or protein-ligand) interactions from rapid reaction kinetic data, *J. Biol. Chem 250*, 4048-4052.

[60] Northrop, D. B. (1998) On the meaning of Km and V/K in enzyme kinetics, *J. Chem. Educ. 75*, 1153.

CHAPTER 3

CONCLUSIONS

NQO is a flavin-dependent enzyme that catalyzes the two-electron reduction of quinones to hydroquinone.[1] The enzyme has a strict preference for NADH as a reducing substrate instead of NADPH.[3] The NADH specificity could have a significant implication in the physiological function of the enzyme, as NADH and NADPH often play very distinct roles within metabolic pathways.[2,3] Previously, the mechanistic and structural properties of NQO were elucidated. This thesis investigates the mechanistic importance of non-catalytic residue in the active site gate of NQO by employing site-directed mutagenesis, UV-visible absorption spectroscopy, rapid reaction kinetics, and steady-state kinetics. The thesis presented the importance of non-catalytic residue in modulating the structural, biophysical, and kinetic properties of NQO.

The crystal structure of NQO showed that Q80 in loop 3 has two distinct conformations in the ligand-free and NAD^+-complex structures, revealing a conformational gating mechanism of Q80 to secure the NAD^+ within the binding pocket.[4] In this thesis, the replacement of Q80 with glycine, leucine, or glutamate through site-directed mutagenesis to study the significance of gate on the ability of NQO to form the enzyme-substrate complex. Comparing steady-state kinetic parameters between mutant and wild type enzymes demonstrated the replacement of Q80 with glycine creates a more open active site gate and decreases the binding affinity of NQO for NADH. On the other hand, mutation of Q80 to a residue of similar length, either nonpolar or charged, such as leucine or glutamate, respectively, demonstrates that a bulky residue better secures NADH in the active site. Therefore, the rates of dissociation constant for NADH binding in the Q80L and Q80E enzymes were reduced compared to the Q80G enzyme and increased compared to the wild type enzyme. The steady-state and rapid reaction kinetics study showed that there is no significant

change in flavin reduction and NQO enzymatic turnover, regardless of residue at position 80 of NQO. The results presented in this study demonstrate that the gating residue Q80 plays a vital role in controlling NADH binding affinity of NQO without impacting the hydride transfer from NADH to flavin.

REFERENCES:

[1] Ball, J., Salvi, F., and Gadda, G. (2016) Functional Annotation of a Presumed Nitronate Monoxygenase Reveals a New Class of NADH:Quinone Reductases*, *J. Biol. Chem. F291*, 21160-21170.

[2] Atia, A., Alrawaiq, N., and Abdullah, A. (2014) A review of NAD(P)H: Quinone oxidoreductase 1 (NQO1); A multifunctional antioxidant enzyme, *J. Appl. Pharm. Sci.4*, 118-122.

[3] Zhao, Q., Yang, X. L., Holtzclaw, W. D., and Talalay, P. (1997) Unexpected genetic and structural relationships of a long-forgotten flavoenzyme to NAD (P) H: quinone reductase (DT-diaphorase), *Proc. Natal. Acad. Sci. 94*, 1669-1674.

[4] Ball, J., Reis, R. A. G., Agniswamy, J., Weber, I. T., and Gadda, G. (2019) Steric hindrance controls pyridine nucleotide specificity of a flavin-dependent NADH:quinone oxidoreductase, *Protein Sci. 28*, 167-175.